In this study, we mapped the epitope for anti-TDP-43 mAb and pAb (Proteintech Group Inc.). We also showed that anti-TDP-43 mAb recognizes human TDP-43, but not mouse TDP-43. Using these antibodies, we investigated the abnormal forms of TDP-43 from ALS and FTLD brains, and found that the antibodies recognized the amino-terminus of the TDP-43 C-terminal fragments of 24–26 kDa. Immunoblot analysis of Sarkosyl-insoluble fractions after treatment of proteases also demonstrated that the epitope is apparently resistant to trypsin and chymotrypsin in the abnormal TDP-43, suggesting that the epitope region is important for the formation of the pathological structure of TDP-43 in ALS and FTLD.

2. Materials and methods

2.1. Construction of plasmids

GFP-tagged TDP-43 C-terminal or N-terminal fragments were constructed as described [23] by amplifying a cDNA encoding full-length TDP-43 by means of PCR and inserting the fragment into the pEGFP-C1 vector (Clontech). To investigate the specificity of TDP-43 mAb for human TDP-43, site-directed mutagenesis of GFP-tagged full-length TDP-43 was carried out to substitute Glu204 to Ala (E204A), Asp205 to Glu (D205E), Arg208 to Gln (R208Q), Glu209 to Gln (E209Q), Ser212 to Cys (S212C), Asp216 to Glu (D216E), and Met218 to Val (M218V), using a site-directed mutagenesis kit (Strategene)(Fig. 4). All constructs were verified by DNA sequencing.

2.2. Antibodies

TDP-43 polyclonal antibody, 10782-2-AP, and TDP-43 monoclonal antibody, 60019-2-Ig, were purchased from Proteintech Group Inc. Anti-GFP monoclonal antibody was purchased from MBL (Nagoya, Japan). A polyclonal antibody specific for phosphorylated TDP-43 (pS409/410) was prepared as described [17].

2.3. Cell culture and expression of plasmids

Human neuroblastoma cell line SH-SY5Y and mouse neuroblastoma cell line Neuro 2a were maintained in appropriate medium as described previously [24,25]. Cells were then transfected with expression plasmids using FuGENE6 (Roche) according to the manufacturer's instructions.

2.4. Immunoblotting

Expressed proteins in cell lysates were separated by 10% SDS–PAGE and transferred onto polyvinylidene difluoride membrane (Millipore, Bedford, MA). After blocking with 3% gelatin, membranes were incubated overnight with primary antibodies (1:1000) at room temperature. After incubation with an appropriate biotinylated secondary antibody, labeling was detected using the ABC system (Vector Lab., Burlingame, CA) coupled with a diaminobenzidine (DAB) reaction intensified with nickel chloride.

2.5. Analysis of abnormal TDP-43 in ALS and FTLD-TDP brain

Brains from two cases with Alzheimer's disease (AD), two with ALS, two with FTLD-TDP (type A), two with FTLD-TDP (type B) and two with FTLD-TDP (type C) were employed in this study. The two AD cases had no TDP-43 pathology. The age, sex, brain weight, and diagnosis are given in Table 1. Sarkosyl-insoluble, urea-soluble fractions were extracted from these brains as previously described [6,9]. The samples were loaded onto 15% polyacrylamide gel and

Table 1
Description of subjects.

Case No.	Diagnosis	Age (years)	Sex	BW (g)
1	AD	65	F	1165
2	AD	70	F	1126
3	ALS	62	M	1230
4	ALS	42	F	1140
5	FTLD-TDP (type A)	71	F	863
6	FTLD-TDP (type A)	66	F	1100
7	FTLD-TDP (type B)	45	M	1260
8	FTLD-TDP (type B)	67	M	1280
9	FTLD-TDP (type C)	67	M	na
10	FTLD-TDP (type C)	59	M	na

BW, brain weight; AD, Alzheimer's disease; ALS, amyotrophic lateral sclerosis; FTLD-TDP, frontotemporal lobar degeneration with TDP-43 pathology; na, not available.

transferred onto a membrane. The membrane was cut in the center of the loaded lane, and the same samples were reacted separately with anti-TDP-43 Abs and pS409/410 as described above.

2.6. Protease treatment of TDP-43

Sarkosyl-insoluble fractions extracted from neocortical regions of the brains were treated with trypsin (at a final concentration of 100 µg/ml, Promega, Madison, USA) or chymotrypsin (at a concentration of 10 µg/ml, Sigma–Aldrich, St. Louis, USA) at 37 °C for 30 min. The reaction was stopped by boiling for 5 min. After centrifuging at 15,000 rpm for 1 min, the samples were analyzed by immunoblotting with anti-TDP-43 pAb and mAb as described above.

3. Results

3.1. Epitope mapping of anti-TDP-43 antibody

Our previous study showed that both TDP-43 mAb and pAb reacted with GFP-tagged TDP-43 C-terminal fragment (GFP-TDP 162–414), but failed to detect GFP-TDP 218–414 [23]. To map the epitope of these antibodies, we expressed a series of GFP-tagged human TDP-43 C-terminal fragments (Fig. 1A) in SH-SY5Y cells and immunoblotted them with the antibodies. Both anti-TDP-43 pAb and mAb detected endogenous human TDP-43 of 43 kDa and exogenous GFP-tagged full-length, 171–414, 181–414, 191–414 and 201–414 TDP-43. However, both antibodies failed to detect 211–414 (Fig. 1A). These results suggest that the epitopes of these antibodies are located within residues 201–210.

To narrow down the epitope structure further, another series of GFP-tagged C-terminal fragments of TDP-43 was expressed in SH-SY5Y cells (Fig. 1B) and tested. Both antibodies reacted with GFP-TDP 203–414, but failed to recognize GFP-TDP 204–414, 205–414 and 207–414 (Fig. 1B), demonstrating that Thr203 forms the N-terminal border of the epitope for both antibodies.

To determine the C-terminus of the epitope, a series of GFP-tagged N-terminal fragments of TDP-43 was expressed and immunoblotted with these antibodies (Fig 1C). Anti-TDP-43 pAb reacted with all of the N-terminal fragments tested, although it stained the 1-212 fragment most strongly. This suggests that one of the pAb epitopes is located at the N-terminal region of TDP-43, in addition to the central epitope. Anti-TDP-43 mAb strongly stained GFP-TDP 1-212, moderately stained GFP-TDP 1-210, and barely stained GFP-TDP 1-209, while it failed to react with GFP 1-208 and 1-207 (Fig. 1C), indicating that Glu209 forms the C-terminus of the epitope for anti-TDP-43 mAb. Thus, anti-TDP-43 mAb recognizes residues 203–209 of human TDP-43.
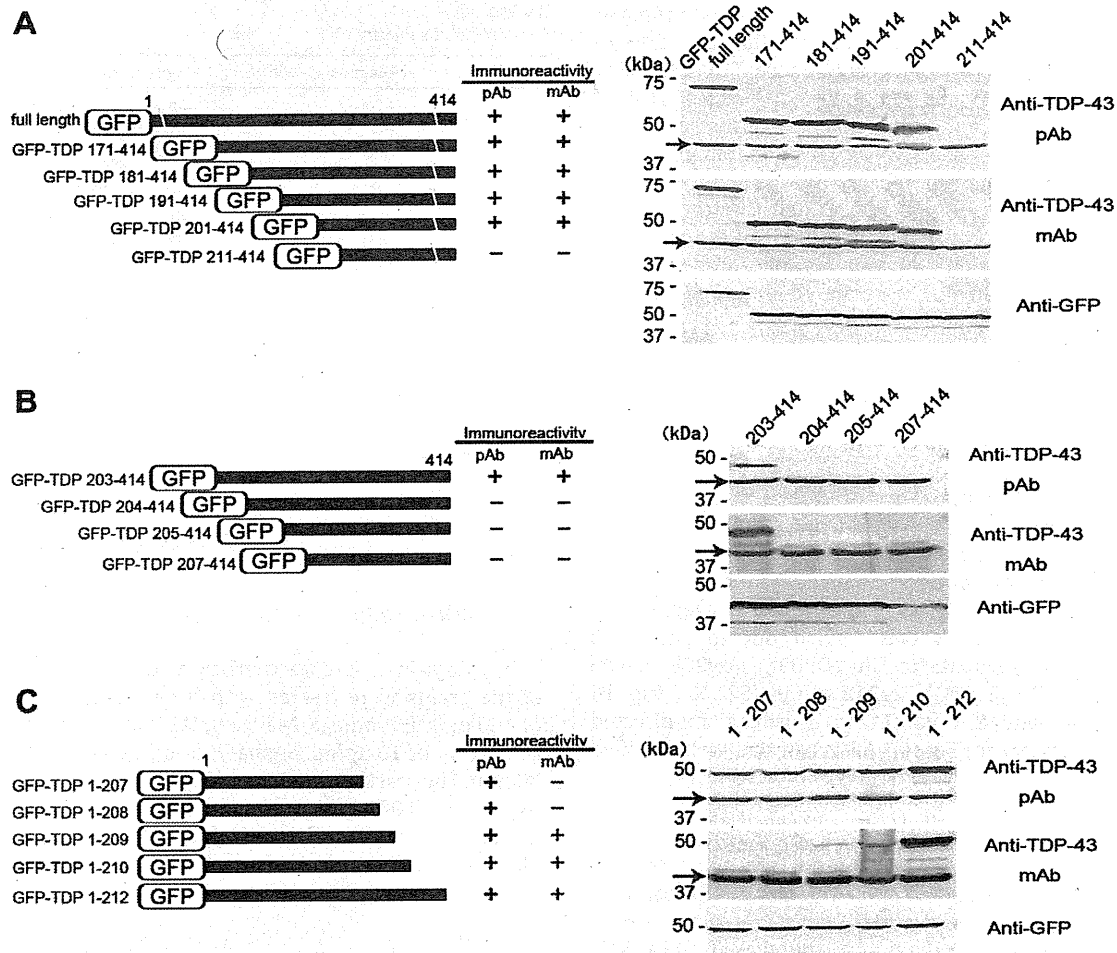
Fig. 1. Epitope mapping of anti-TDP-43 polyclonal and monoclonal antibodies. (A) Schematic diagram of GFP-tagged full-length TDP-43 (GFP-TDP) and the C-terminal fragments. Immunoblot analyses of GFP-TDP and the C-terminal fragments in SH-SY5Y cells. Both mAb and pAb reacted with GFP-TDP and the C-terminal fragments, except for 211–414. The anti-GFP antibody recognizes all the proteins expressed. (B) Further epitope mapping of anti-TDP-43 antibodies. Immunoblot analyses of the GFP tagged C-terminal fragments of TDP-43. Both mAb and pAb reacted with 203–414, but failed to recognize 204–414, 205–414, and 207–414. The anti-GFP antibody recognizes all of the fragments. (C) Epitope mapping of the C-terminus recognized by anti-TDP-43 polyclonal and monoclonal antibodies. Immunoblot analyses of GFP-TDP and N-terminal fragments in SH-SY5Y cells. Anti-TDP-43 pAb reacted with all of the N-terminal fragments, although it stained 1-212 fragment most strongly. In contrast, anti-TDP-43 mAb strongly stained GFP-TDP 1-212, moderately stained GFP-TDP 1-210, and barely stained GFP-TDP 1-209, while it failed to react with GFP 1-208 and 1-207. The anti-GFP antibody recognized all of the fragments equally. The arrows indicate endogenous TDP-43 in SH-SY5Y cells.

3.2. Amino acid sequence differences between human and mouse TDP-43

The anti-TDP-43 mAb reacted with endogenous TDP-43 of human neuroblastoma SH-SY5Y cells, but not with TDP-43 of mouse neuroblastoma Neuro2a cells (Fig. 1B, 1C, 2B). Similarly, the mAb recognized TDP-43 in human brain extract, but failed to detect TDP-43 in mouse brain extract, suggesting that the mAb does not recognize mouse TDP-43 (data not shown). The absence of reactivity with mouse TDP-43 is explained by the sequence differences around the epitope between human and mouse TDP-43 (Fig. 2A). Each different amino acid of human TDP-43 was substituted to that of mouse TDP-43. The mutated proteins were expressed in Neuro2a cells and immunoreactivity with anti-TDP-43 mAb was examined. Substitution of D216 to E and M218 to V did not affect the immunoreactivity (Fig. 2B), whereas substitutions of E204 to A, D205 to E, and R208 to Q abolished the immunoreactivity of anti-TDP-43 mAb, indicating that these residues are necessary for recognition by the mAb. Anti-TDP-43 pAb reacted with these mutants, although a marked

decrease in immunoreactivity was observed in the cases of E204A, D205A, R208Q, and S212C.

3.3. Biochemical analysis of abnormal TDP-43 in ALS and FTLD brains with anti-TDP-43 mAb

On immunoblots of Sarkosyl-insoluble fractions extracted from the brain of patients with ALS and FTLD-TDP (type A), the anti-TDP-43 mAb detected phosphorylated full-length TDP-43 at 45 kDa, two bands around 25 kDa and high-molecular-weight smears, in addition to the normal TDP-43 band at 43 kDa, which can also be detected in control cases. Immunoblot analysis of the split membrane with a phosphorylation-dependent anti-TDP-43 antibody pS409/410 revealed that the two bands around 25 kDa stained with the mAb corresponded to the C-terminal fragments of 24 and 26 kDa recognized by pS409/410 (Fig. 3)[17]. These results demonstrated that these 24 and 26 kDa C-terminal fragments contain the epitope of the mAb, residues 203–209, and that the cleavage sites of these C-terminal fragments are located at the N-terminal side of Thr203.

A

201   220

H. Sap. · · · DMTEDELREFFSQYGDVMDV · · ·
             ***   ** ** *** * **
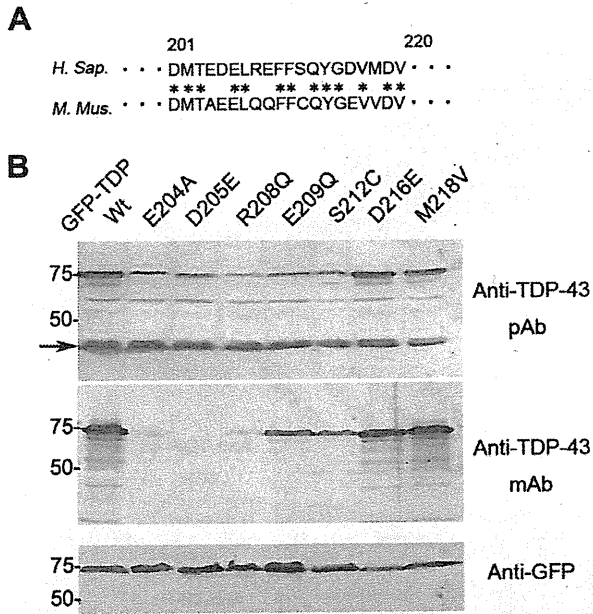M. Mus. · · · DMTAEELQQFFCQYGEVVDV · · ·

B

Fig. 2. Alignment of human and mouse TDP-43 (A) and immunoblot analyses of mutated TDP-43 with anti-TDP-43 antibodies. (A) The amino acid sequences of human (upper) and mouse (lower) TDP-43 around the epitope of anti-TDP-43 mAb. The asterisks show identical amino acids. (B) Immunoblot analyses of GFP-TDP wild type (Wt) and GFP-TDP mutants expressed in Neuro2a cells. Substitution of D216 to E and M218 to V did not affect the immunoreactivity, whereas substitutions of E204 to A, D205 to E, and R208 to Q, abolished the immunoreactivity of anti-TDP-43 mAb. Anti-TDP-43 pAb reacted with all these mutants, although markedly decreased immunoreactivities were observed in E204A, D205A, R208Q, and S212C. The arrows indicated endogenous TDP-43 in Neuro2A cells. Note that endogenous mouse TDP-43 in Neuro 2a cells was not recognized by anti-TDP-43 mAb.
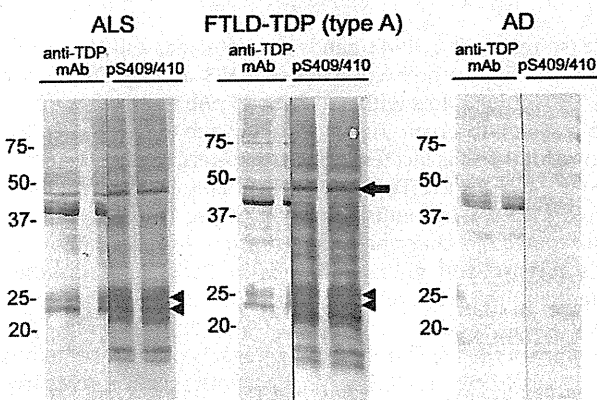

Fig. 3. Immunoblot analyses of Sarkosyl-insoluble fractions from ALS, FTLD-TDP (type A), and AD brains with anti-TDP-43 monoclonal antibody and phosphorylation-dependent anti-TDP-43 antibody, pS409/410. With pS409/410, fragments of approximately 45 kDa and 18–26 kDa, as well as smearing, were detected. The banding pattern of 18–26 kDa fragments showed three major bands at 23, 24, and 26 kDa, and 2 minor bands at 18 and 19 kDa, with the 24 kDa band being the most intense. In addition to the normal full-length TDP-43 at 43 kDa, anti-TDP-43 mAb labeled phosphorylated full-length TDP-43 at 45 kDa, high-molecular-weight smears and two bands at 26 kDa and 24 kDa (arrowheads), which were not seen in the AD case. The two bands corresponded to the major 26 and 24 kDa bands were detected with pS409/410.

3.4. The epitope of these TDP-43 antibodies constitute part of protease-resistant core domain of TDP-43 in ALS and FTLD brains

In order to characterize the epitope further, we treated the Sarkosyl-insoluble fractions extracted from brains of patients with proteases and analyzed them with these antibodies. Without pro-

tease treatment, both antibodies strongly stained normal full-length TDP-43 of 43 kDa in all cases examined including AD cases which were without TDP-43 pathology. In ALS and FTLD-TDP cases, phosphorylated full-length TDP-43 of 45 kDa (Fig 4A, arrows) and the ~25 kDa fragments (Fig 4A, arrow heads) were detected with these antibodies. After trypsin treatment, the full-length band of TDP-43 was disappeared and the protease-resistant fragments around 25 kDa (Fig 4B, white arrows) and smearing substances appeared in the ALS and FTLD-TDP cases. Similarly, after chymotrypsin treatment, protease-resistant triplet bands of 16, 20 and 25 kDa (Fig 4C, white arrow heads) and smearing substances were clearly detected in ALS and FTLD-TDP-cases with the mAb, while no such bands were seen in AD cases. On blot with the pAb, multiple bands were detected in addition to the triplet, and some of these bands were also detected in AD cases, suggesting that the pAb stained some normal fragments in addition to the abnormal TDP-43 bands. In the cases examined, apparent difference was not detected in these trypsin-resistant and chymotrypsin-resistant bands detected among the clinicopathological phenotypes of the diseases. By proteinase K treatment, immunoreactivities with these antibodies were completely abolished (data not shown), suggesting that the epitope is not entirely resistant to any proteases. However, it is obvious that the epitope of the TDP-43 deposited in the patients is fairly protease-resistant compared to the normal protein. These results indicate that the epitope of the mAb (residues 203–209 of TDP-43) constitute part of the protease-resistant domain of TDP-43 which determine a common characteristic of the abnormal TDP-43 in both ALS and FTLD-TDP.

4. Discussion

This is the first analysis of the epitopes of Proteintech's anti-TDP-43 polyclonal and monoclonal antibodies, which have often been used to research TDP-43 proteinopathies since 2006 [6,7]. We demonstrated that anti-TDP-43 mAb specifically recognizes residues 203–209 of human TDP-43, which form a part of the second RNA-recognition motif (RRM2, residues 193–257) of normal TDP-43 [26], but constitute part of the protease-resistant core domain of TDP-43 aggregates that determine the common characteristic of abnormal TDP-43 in ALS and FTLD-TDP-43.

RRM2 is a functional domain with distinct RNA/DNA binding characteristics. The anti-TDP-43 mAb recognized human TDP-43, but not mouse TDP-43. Site-directed mutagenesis and subsequent immunoblot analysis revealed that Glu204, Asp205 and Arg208 residues in human TDP-43 are important for the specific recognition by the mAb (Fig. 2). In fact, human TDP-43 shares 98.5% homology with mouse TDP-43 at the amino acid level, but the RRM2 domain has only 66% homology.

We also showed that one of the major epitopes of the pAb is located in almost the same region at that of the mAb (Fig. 1), although the pAb also recognizes the N-terminal region of TDP-43. Recently, TDP-43 transgenic mice overexpressing human TDP-43 have been produced as animal models of TDP-43 proteinopathy [27]. However, abnormal TDP-43 pathologies in these mice are very rare, so new transgenic or other animal models that develop abundant TDP-43 pathology are still required. Since the TDP-43 mAb recognizes human TDP-43, but not mouse TDP-43, it will be a useful reagent for the characterization of mouse lines transgenic for human TDP-43, together with phosphorylation-dependent antibodies.

Biochemical analyses of TDP-43 proteinopathies have demonstrated that abnormally phosphorylated full-length and C-terminal fragments of TDP-43 are the major species in the inclusions. The band patterns of the C-terminal fragments at 18–26 kDa are closely correlated with the clinicopathological subtypes of TDP-43 proteinopathies [17]. In addition, most of the pathogenic mutations
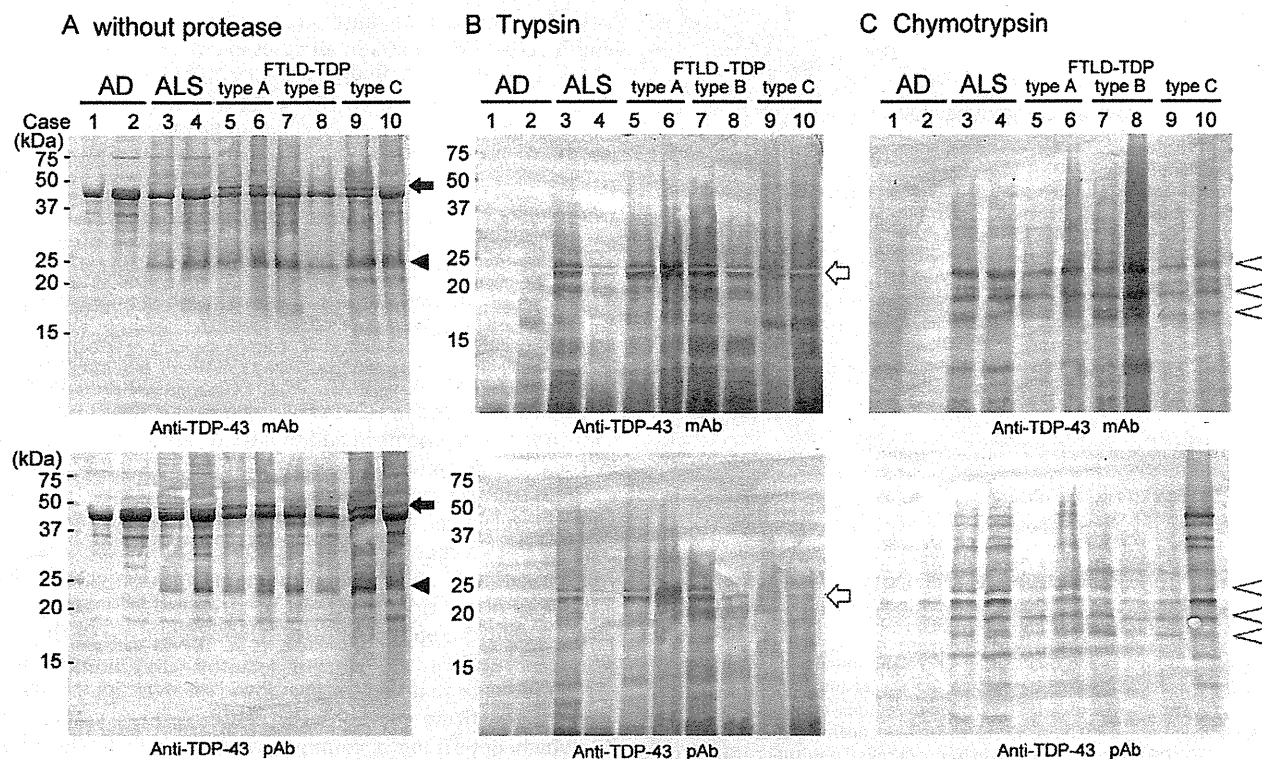
Fig. 4. Immunoblot analysis of Sarkosyl-insoluble fractions from AD and TDP-43 proteinopathies before and after protease treatment. (A) Without protease treatment, normal TDP-43 of 43 kDa was detected with these antibodies in all cases examined. In the ALS and FTLD-TDP cases, phosphorylated full-length TDP-43 of 45 kDa (arrows), high-molecular-weight smears, and the 24–26 kDa fragments (arrow heads) were detected in addition to the normal TDP-43. (B) Upon trypsin treatment, full-length TDP-43 disappeared, and the protease-resistant ~25 kDa fragments (white arrows) and smears appeared in ALS and FTLD-TDP cases, but not in AD cases. (C) After chymotrypsin treatment, triplet bands (white arrowheads) were detected in ALS and FTLD-TDP cases with the mAb and multiple bands were detected with pAb, whereas such immunoreactivities were hardly detected in AD cases.

are found in the C-terminal half of the TDP-43 [13–16]. Therefore, misfolding or structural alteration of the C-terminal half of TDP-43 seems to be the key to the pathogenesis of TDP-43 proteinopathies. By mass spectrometric analysis of the 23 kDa band in Sarkosyl-insoluble fraction from FTLD-TDP (type A), we identified the cleavage site as the N-terminus of Asp219 [23]. Another group reported cleavage at Asp208, based on N-terminal sequencing of urea extracts of FTLD-TDP brain [28]. However, the cleavage sites of the other major C-terminal fragments of 24 and 26 kDa have not been determined yet. In this study, we showed that the pathological TDP-43 C-terminal fragments of 24 and 26 kDa in ALS and FTLD-TDP type A contain the epitope of anti-TDP-43 mAb, residues 203–209, by comparing the immunoblotting results with those using pS409/410 (Fig. 3). This result suggests that the cleavage sites of pathological TDP-43 C-terminal fragments in ALS and FTLD-TDP are located at the N-terminal side of Thr203. Although the mechanisms of generation of the C-terminal fragments are still controversial, the presence of multiple cleavage sites suggests that cleavage may occur after the aggregation or assembly of TDP-43.

Structural or conformational changes in the proteins are thought to be the most important in protein aggregation in these neurodegenerative diseases. To analyze the conformational change in the epitope of TDP-43 from normal to the abnormal states further, we treated the Sarkosyl-insoluble TDP-43 with trypsin or chymotrypsin, and immunoblotted with these antibodies. The protease-resistant TDP-43 bands and smears were detected in ALS and all subtypes of FTLD-TDP with these anti-TDP-43 antibodies (Fig. 4), while no such bands were seen in AD cases. These demonstrate that the epitope is protease-resistant in the abnormal TDP-43 but not in normal TDP-43. Using an antibody pS409/410 that recognizes the C-terminal phosphorylation sites, some

protease-resistant TDP-43 bands are detected, and the band patterns are slightly different between ALS and FTLD-TDP type C [29]. On immunoblots with anti-TDP-43 pAb and mAb, such difference was not observed. This is probably due to that the epitope of the mAb and pAb is located in the amino-terminus of the protease-resistant core of the TDP-43, whereas epitope of the pS409/410 located in the C-terminus. Similar protease-resistant bands have been reported in abnormal prion in prion diseases, tau in Alzheimer's disease and alpha-synuclein in Parkinson's disease and dementia with Lewy bodies. Biochemical studies in these proteinopathies suggested that the protease-resistant bands represent the core domains of the filamentous aggregates of these proteins with cross-β structures [30–32]. By analogy with these proteins we propose that these protease-resistant C-terminal fragments represent the core of the filamentous aggregates of TDP-43. Since the epitope of the mAb and pAb are determined to locate at residues 203–209, this may be important in the formation of a core region of pathological TDP-43 aggregates which is common in all TDP-43 proteinopathies. Finally, the protease treatment used in this study may be useful for detection of the abnormal TDP-43 in brains of patients, animal models, culture cells and in vitro models with these anti-TDP-43 antibodies more specifically, as used for detection of abnormal prion proteins.

Acknowledgments

References

[1] Y.M. Ayala, T. Misteli, F.E. Baralle, TDP-43 regulates retinoblastoma protein phosphorylation through the repression of cyclin-dependent kinase 6 expression, Proc. Natl. Acad. Sci. U.S.A. 105 (2008) 3785–3789.

[2] Y.M. Ayala, F. Pagani, F.E. Baralle, TDP43 depletion rescues aberrant CFTR exon 9 skipping, FEBS Lett. 580 (2006) 1339–1344.

[3] E. Buratti, F.E. Baralle, Multiple roles of TDP-43 in gene expression, splicing regulation, and human disease, Front. Biosci. 13 (2008) 867–878.

[4] S.H. Ou, F. Wu, D. Harrich, et al., Cloning and characterization of a novel cellular protein, TDP-43, that binds to human immunodeficiency virus type 1 TAR DNA sequence motifs, J. Virol. 69 (1995) 3584–3596.

[5] I.F. Wang, N.M. Reddy, C.K. Shen, Higher order arrangement of the eukaryotic nuclear bodies, Proc. Natl. Acad. Sci. U.S.A. 99 (2002) 13583–13588.

[6] T. Arai, M. Hasegawa, H. Akiyama, et al., TDP-43 is a component of ubiquitin-positive tau-negative inclusions in frontotemporal lobar degeneration and amyotrophic lateral sclerosis, Biochem. Biophys. Res. Commun. 351 (2006) 602–611.

[7] M. Neumann, D.M. Sampathu, L.K. Kwong, et al., Ubiquitinated TDP-43 in frontotemporal lobar degeneration and amyotrophic lateral sclerosis, Science 314 (2006) 130–133.

[8] T. Arai, I.R. Mackenzie, M. Hasegawa, et al., Phosphorylated TDP-43 in Alzheimer's disease and dementia with Lewy bodies, Acta Neuropathol. (Berl) 117 (2009) 125–136.

[9] M. Hasegawa, T. Arai, H. Akiyama, et al., TDP-43 is deposited in the Guam parkinsonism-dementia complex brains, Brain 130 (2007) 1386–1394.

[10] C.F. Tan, M. Yamada, Y. Toyoshima, et al., Selective occurrence of TDP-43-immunoreactive inclusions in the lower motor neurons in Machado-Joseph disease, Acta Neuropathol. (Berl) 118 (2009) 553–560.

[11] Y. Toyoshima, H. Tanaka, M. Shimohata, et al., Spinocerebellar ataxia type 2 (SCA2) is associated with TDP-43 pathology, Acta Neuropathol. (Berl) 122 (2011) 375–378.

[12] O. Yokota, Y. Davidson, E.H. Bigio, et al., Phosphorylated TDP-43 pathology and hippocampal sclerosis in progressive supranuclear palsy, Acta Neuropathol. (Berl) 120 (2010) 55–66.

[13] E. Kabashi, P.N. Valdmanis, P. Dion, et al., TARDBP mutations in individuals with sporadic and familial amyotrophic lateral sclerosis, Nat. Genet. 40 (2008) 572–574.

[14] J. Sreedharan, I.P. Blair, V.B. Tripathi, et al., TDP-43 mutations in familial and sporadic amyotrophic lateral sclerosis, Science 319 (2008) 1668–1672.

[15] A. Tamaoka, M. Arai, M. Itokawa, et al., TDP-43 M337V mutation in familial amyotrophic lateral sclerosis in Japan, Intern. Med. 49 (2010) 331–334.

[16] I.R. Mackenzie, R. Rademakers, M. Neumann, TDP-43 and FUS in amyotrophic lateral sclerosis and frontotemporal dementia, Lancet Neurol. 9 (2010) 995–1007.

[17] M. Hasegawa, T. Arai, T. Nonaka, et al., Phosphorylated TDP-43 in frontotemporal lobar degeneration and amyotrophic lateral sclerosis, Ann. Neurol. 64 (2008) 60–70.

[18] I.R. Mackenzie, E.H. Bigio, P.G. Ince, et al., Pathological TDP-43 distinguishes sporadic amyotrophic lateral sclerosis from amyotrophic lateral sclerosis with SOD1 mutations, Ann. Neurol. 61 (2007) 427–434.

[19] M. Neumann, L.K. Kwong, A.C. Truax, et al., TDP-43-positive white matter pathology in frontotemporal lobar degeneration with ubiquitin-positive inclusions, J. Neuropathol. Exp. Neurol. 66 (2007) 177–183.

[20] H. Zhang, C.F. Tan, F. Mori, et al., TDP-43-immunoreactive neuronal and glial inclusions in the neostriatum in amyotrophic lateral sclerosis with and without dementia, Acta Neuropathol. (Berl) 115 (2008) 115–122.

[21] M. Neumann, I.R. Mackenzie, N.J. Cairns, et al., TDP-43 in the ubiquitin pathology of frontotemporal dementia with VCP gene mutations, J. Neuropathol. Exp. Neurol. 66 (2007) 152–157.

[22] H.X. Zhang, K. Tanji, F. Mori, et al., Epitope mapping of 2E2-D3, a monoclonal antibody directed against human TDP-43, Neurosci. Lett. 434 (2008) 170–174.

[23] T. Nonaka, F. Kametani, T. Arai, et al., Truncation and pathogenic mutations facilitate the formation of intracellular aggregates of TDP-43, Hum. Mol. Genet. 18 (2009) 3353–3364.

[24] T. Nonaka, T. Arai, E. Buratti, et al., Phosphorylated and ubiquitinated TDP-43 pathological inclusions in ALS and FTLD-U are recapitulated in SH-SY5Y cells, FEBS Lett. 583 (2009) 394–400.

[25] Y. Nishimoto, D. Ito, T. Yagi, et al., Characterization of alternative isoforms and inclusion body of the TAR DNA-binding protein-43, J. Biol. Chem. 285 (2010) 608–619.

[26] E. Buratti, F.E. Baralle, Characterization and functional implications of the RNA binding properties of nuclear factor TDP-43, a novel splicing regulator of CFTR exon 9, J. Biol. Chem. 276 (2001) 36337–36343.

[27] H. Wils, G. Kleinberger, J. Janssens, et al., TDP-43 transgenic mice develop spastic paralysis and neuronal inclusions characteristic of ALS and frontotemporal lobar degeneration, Proc. Natl. Acad. Sci. U.S.A. 107 (2010) 3858–3863.

[28] L.M. Igaz, L.K. Kwong, A. Chen-Plotkin, et al., Expression of TDP-43 C-terminal Fragments in Vitro Recapitulates Pathological Features of TDP-43 Proteinopathies, J. Biol. Chem. 284 (2009) 8516–8524.

[29] M. Hasegawa, T. Nonaka, H. Tsuji, et al., Molecular Dissection of TDP-43 Proteinopathies, J. Mol. Neurosci. 45 (2011) 480–485.

[30] J. Collinge, K.C. Sidle, J. Meads, et al., Molecular analysis of prion strain variation and the aetiology of 'new variant' CJD, Nature 383 (1996) 685–690.

[31] H. Miake, H. Mizusawa, T. Iwatsubo, et al., Biochemical characterization of the core structure of alpha-synuclein filaments, J. Biol. Chem. 277 (2002) 19213–19219.

[32] M. Novak, J. Kabat, C.M. Wischik, Molecular characterization of the minimal protease resistant tau unit of the Alzheimer's disease paired helical filament, EMBO J. 12 (1993) 365–370.

ORIGINAL PAPER

Phosphorylated TDP-43 in Alzheimer's disease and dementia with Lewy bodies

Tetsuaki Arai · Ian R. A. Mackenzie · Masato Hasegawa · Takashi Nonoka ·
Kazhuhiro Niizato · Kuniaki Tsuchiya · Shuji Iritani · Mitsumoto Onaya ·
Haruhiko Akiyama

Abstract Phosphorylated and proteolytically cleaved TDP-43 is a major component of the ubiquitin-positive inclusions in the most common pathological subtype of frontotemporal lobar degeneration (FTLD-U). Intracellular accumulation of TDP-43 is observed in a subpopulation of patients with other dementia disorders, including Alzheimer's disease (AD) and dementia with Lewy bodies (DLB). However, the pathological significance of TDP-43 pathology in these disorders is unknown, since biochemical features of the TDP-43 accumulated in AD and DLB brains, especially its phosphorylation sites and pattern of fragmentation, are still unclear. To address these issues, we performed immunohistochemical and biochemical analyses of AD and DLB cases, using phosphorylation-dependent anti-TDP-43 antibodies. We found a higher frequency of pathological TDP-43 in AD (36–56%) and in DLB (53–60%) than previously reported. Of the TDP-43-positive cases, about 20–30% showed neocortical TDP-43 pathology resembling the FTLD-U subtype associated with progranulin gene (*PGRN*) mutations. Immunoblot analyses of the sarkosyl-insoluble fraction from cases with neocortical TDP-43 pathology showed intense staining of several low-molecular-weight bands, corresponding to C-terminal fragments of TDP-43. Interestingly, the band pattern of these C-terminal fragments in AD and DLB also corresponds to that previously observed in the FTLD-U subtype associated with *PGRN* mutations. These results suggest that the morphological and biochemical features of TDP-43 pathology are common between AD or DLB and a specific subtype of FTLD-U. There may be genetic factors, such as mutations or genetic variants of *PGRN* underlying the co-occurrence of abnormal deposition of TDP-43, tau and α-synuclein.

Keywords Phosphorylation · Fragmentation · Frontotemporal lobar degeneration · Progranulin · Tau · Alpha-synuclein · TDP-43

T. Arai (✉) · H. Akiyama
Department of Psychogeriatrics,
Tokyo Institute of Psychiatry,
Tokyo Metropolitan Organization for Medical Research,
2-1-8 Kamikitazawa, Setagaya-ku, Tokyo 156-8585, Japan
e-mail: arai@prit.go.jp

I. R. A. Mackenzie
Department of Pathology,
Vancouver General Hospital, 855 West 12th Avenue,
Vancouver, BC V5Z 1M9, Canada

M. Hasegawa · T. Nonoka
Department of Molecular Neurobiology,
Tokyo Institute of Psychiatry,
Tokyo Metropolitan Organization for Medical Research,
2-1-8 Kamikitazawa, Setagaya-ku,
Tokyo 156-8585, Japan

K. Niizato
Department of Psychiatry,
Tokyo Metropolitan Matsuzawa Hospital,
2-1-1 Kamikitazawa, Setagaya-ku, Tokyo 156-0057, Japan

K. Tsuchiya
Department of Laboratory Medicine and Pathology,
Tokyo Metropolitan Matsuzawa Hospital, 2-1-1 Kamikitazawa,
Setagaya-ku, Tokyo 156-0057, Japan

S. Iritani
Department of Psychiatry,
Nagoya University Graduate School of Medicine,
Nagoya, Aichi 466-8550, Japan

M. Onaya
Department of Neuropsychiatry,
National Shimofusa Mental Hospital, Chiba 266-0007, Japan

🙋 Springer

Introduction

TAR DNA-binding protein of M_r 43 kDa (TDP-43) is a major component of the tau-negative and ubiquitin-positive inclusions that characterize the most common pathological subtype of frontotemporal lobar degeneration (FTLD-U) and amyotrophic lateral sclerosis (ALS) [2, 9, 24, 31, 32, 38]. Several genes and chromosomal loci, including the progranulin gene (PGRN) [4, 8], valosin-containing protein gene (VCP) [42] and an unidentified gene at chromosome 9p [28, 41], have been reported to be associated with familial forms of FTLD-U. Recent findings of various missense mutations of TDP-43 gene (TARDBP) in familial and sporadic ALS cases prove the essential role of abnormal TDP-43 in neurodegeneration [12, 20, 37, 40, 43]. These disorders are now collectively referred to as TDP-43 proteinopathies [2, 9, 31, 32].

Ubiquitin- and TDP-43-positive pathological inclusions found in FTLD-U include neuronal cytoplasmic inclusions (NCIs), dystrophic neurites (DNs), neuronal intranuclear inclusions (NIIs), and glial cytoplasmic inclusions [2, 25, 26, 32, 35]. Based on the cerebral ubiquitin immunohisto-chemistry, FTLD-U was classified into three subtypes by Sampathu et al. [35] and Mackenzie et al. [25]. Unfortunately, the numbering schemes used in these two systems do not match. Type 1 by Sampathu et al. or Type 2 by Mackenzie et al. is characterized by DNs with few NCIs and no NIIs. Type 2 by Sampathu et al. or Type 3 by Mackenzie et al. has numerous NCIs with few DNs and no NIIs. Type 3 by Sampathu et al. or Type 1 by Mackenzie et al. has numerous NCIs and DNs and occasional NIIs. This is the pattern found in all cases of FTD caused by mutations in PGRN [7, 25]. Recently, Cairns et al. [7] drew these two systems together into a unified scheme, and added familial FTLD-U with VCP mutations as Type 4, which has numerous NIIs and DNs with few NCIs. Since they adopted the numbering system by Sampathu et al. in their consensus paper, we will use that for the rest of this paper.

Biochemical analyses of the detergent-insoluble fraction extracted from brains of patients afflicted with FTLD-U showed that TDP-43 accumulated in these pathological structures is composed of abnormal C-terminal fragments that are phosphorylated and ubiquitinated [2, 32]. Using antibodies specific for phosphorylated TDP-43 (pTDP-43), made by ourselves, we previously identified several phosphorylation sites in the C-terminal region of the TDP-43 that accumulates in FTLD-U brains [14]. Furthermore, we found a close relationship between the pathological subtypes of FTLD-U and the immunoblot pattern of phosphorylated C-terminal fragments of TDP-43, suggesting that proteolytic processing may be crucial in TDP-43 proteinopathy [14].

Recently, immunohistochemical examination, using commercially available phosphorylation-independent anti-TDP-43 antibodies, has demonstrated abnormal intracellular accumulation of TDP-43 in neurodegenerative disorders other than FTLD-U and ALS. These include Alzheimer's disease (AD), dementia with Lewy bodies (DLB), Pick's disease, hippocampal sclerosis, corticobasal degeneration, Huntington disease and argyrophilic grain disease [1, 11, 15, 17, 19, 23, 30, 36, 39]. However, the pathological significance of TDP-43 accumulation in these disorders is unclear, since it takes place only in a subpopulation of the patients with most of these disorders. Moreover, although the morphology of the TDP-43 positive structures has been described, the biochemical features of accumulated TDP-43, especially its phosphorylation sites and fragmentation, are still unclear in these disorders. To address these issues, in the present study, we performed detailed immunohisto-chemical and biochemical analyses of TDP-43 in cases of AD and DLB, using our phosphorylation-dependent anti-TDP-43 antibodies. We find a relatively higher frequency of TDP-43 deposition in AD and DLB than previously reported. When TDP-43 pathology occurs in the neocortex of cases with AD and DLB, the pattern is Type 3. In these cases, the accumulated TDP-43 demonstrates abnormal C-terminal phosphorylation and fragmentation. These results suggest the presence of a common mechanism underlying the abnormal processing and accumulation of TDP-43 in AD, DLB and a specific subtype of FTLD-U.

Materials and methods

Materials

We studied two independent series of cases (Table 1). The first was comprised of 53 AD cases and 15 DLB cases from the institutional collections at the Department of Psychogeriatrics, Tokyo Institute of Psychiatry in Japan. The second series included 25 AD cases and 10 DLB cases from the Canadian Collaborative Cohort of Related Dementia (ACCORD) study, a well-characterized memory clinic population, prospectively followed to death [10]. The second series provided validation of the findings from the first series, included examination of some additional neuroanatomical regions not available in the first series and tested whether similar results could be obtained by using more traditional immunohistochemical methodology.

Neuropathological diagnoses of AD and DLB were made in accordance with published guidelines [27, 33] for both series. Two cases from the first series and one case from the second series had little AD pathology, corresponding to the pure form of diffuse Lewy body disease (DLBD) [21].

Table 1 Demographics and pathology of all cases employed in this study

	Alzheimer's disease						Dementia with Lewy bodies					
	First series (N = 53)			Second series (N = 25)			First series (N = 15)			Second series (N = 10)		
	TDP-43 positive	TDP-43 negative	P value	TDP-43 positive	TDP-43 negative	P value	TDP-43 positive	TDP-43 negative	P value	TDP-43 positive	TDP-43 negative	P value
Number of cases (%)	19 (36%)	34 (64%)		14 (56%)	11 (44%)		8 (53%)	7 (47%)		6 (60%)	4 (40%)	
Mean age at death ± SD (years)	82.8 ± 7.5	78.8 ± 10.7	0.16	81.2 ± 7.0	72.7 ± 9.2	0.015*	73.5 ± 12.8	81.7 ± 6.5	0.15	76.3 ± 7.4	71.0 ± 9.5	0.35
Sex, M:F	11:8	20:14	0.95	8:6	5:6	0.56	6:2	5:2	>0.99	4:2	3:1	>0.99
Median Braak NFT stage (25th, 75th percentile)	5 (5.0, 6.0)	5 (4.0, 5.0)	0.027*	6 (6.0, 6.0)	6 (6.0, 6.0)	0.7	4 (3.0, 6.0)	4 (3.25, 4.0)	0.54	4.5 (2.0, 6.0)	6 (6.0, 6.0)	0.11
Brain weight ± SD (g)	1,117 ± 162	1,116 ± 137	0.98	NA	NA		1,123 ± 151	1,144 ± 146	0.79	NA	NA	

Immunohistochemistry

For the first series, small blocks of brain were dissected at autopsy and fixed in 4% paraformaldehyde (PFA) in 0.1 M phosphate buffer (pH 7.4) for 2 days. Following the cryo-protection in 15% sucrose in 0.01 M phosphate-buffered saline (PBS, pH 7.4), blocks were cut on a freezing microtome at 30 μm thickness. The free floating sections were incubated with 0.5% H_2O_2 for 30 min to eliminate endogenous peroxidase activity in the tissue. After washing with PBS containing 0.3% Triton X-100 (Tx-PBS) for 30 min, sections were blocked with 10% normal serum, and then incubated with the primary antibody for 72 h in the cold. Following treatment with the appropriate secondary antibody, labeling was detected using the avidin–biotinylated HRP complex (ABC) system (Vector Laboratories, Burlingame, CA) coupled with a diaminobenzidine (DAB) reaction to yield a brown precipitate, or with a DAB reaction intensified with nickel ammonium sulfate to yield a dark purple precipitate, as previously described [2, 3, 13, 14]. For the second series, immunohistochemistry was performed on 5-μm-thick sections of formalin-fixed, paraffin-embedded tissue, using the Ventana BenchMark® XT automated staining system (Ventana, Tuscon, AZ), as previously described [25]. Prior to immunostaining, sections underwent microwave antigen retrieval for 13 min in citrate buffer, pH 6.0. Immunoreactions were developed with aminoethylcarbizole (AEC).

In the first series, the presence and severity of pTDP-43 immunoreactivity was assessed in amygdala (where available), hippocampus, entorhinal cortex and temporal neocortex. More extensive anatomical sampling was available in the second series allowing pathology to be assessed in the amygdala, hippocampus, entorhinal cortex, cingulate gyrus, temporal neocortex, frontal neocortex and parietal neocortex. pTDP-43 pathology was semiquantitatively scored based on a five-point grading scale (−, none; ±, rare; +, mild; ++, moderate; +++, severe). The primary antibodies used in this study and their dilutions are summarized in Table 2. Only pTDP-43-specific antibodies (pS409/410 and pS403/404) were employed in the first series, while both phosphorylation-independent commercial anti-TDP-43 antibody and pTDP-43-specific antibodies were employed in the second series. In the second series, all the same cases were stained with both antibodies but the pTDP-43-specific antibodies often stained a greater amount of pathology.

Statistical analyses

Unpaired Student's t tests were used to analyze differences between groups for age and brain weights, whereas the Braak stage score was analyzed with Mann–Whitney

Table 2 Antibodies used in this study

Antibody	Type	Source	Dilution
Phosphorylation-independent anti-TDP-43			
Anti-TDP-43	Rabbit polyclonal (affinity purified)	ProteinTech, Chicago, IL	1:1,000 (IB, IHC-P)
Phosphorylation-dependent anti-TDP-43			
pS409/410	Rabbit serum	a	1:1,000 (IB, IHC-P), 1:10,000 (IHC-F), 1:5,000 (IF)
pS403/404	Rabbit serum	a	1:1,000 (IB, IHC-P), 1:10,000 (IHC-F), 1:5,000 (IF)
Anti-tau			
AT8	Mouse monoclonal	Innogenetics, Gent, Belgium	1:2,000 (IHC-P), 1:100 (IF)
Anti-α-synuclein			
pα#64	Mouse monoclonal	Wako Chemical, Osaka, Japan	1:3,000 (IF)
Anti-α-synuclein	Mouse monoclonal	Invitrogen, Burlington, ON, Canada	1:10,000 (IHC-P)
Anti-amyloid β protein			
6F3D	Mouse monoclonal	DAKO, Mississauga, ON, Canada	1:100 (IHC-P)

IB immunoblotting, *IHC-P* immunohistochemistry in paraffin-embedded sections, *IHC-F* immunohistochemistry in free-floating sections, *IF* immunofluorescence

[a] Made by ourselves [14]

U test. χ^2 and Fisher's exact test were used to analyze the difference between groups for sex.

Confocal microscopy

For double labeling immunofluorescence for pTDP-43 and phosphorylated tau in AD or for pTDP-43 and phosphorylated α-synuclein in DLB, 4% PFA-fixed and free floating sections from the first series were used. The sections were incubated overnight at 4°C in a cocktail of pS409/410 or pS403/404 and AT8 or pα#64. After washing with Tx-PBS for 30 min, sections were incubated for 2 h at room temperature in a cocktail of Fluorescein isothiocianate (FITC)-conjugated goat anti-mouse IgG (1:100, Millipore, Temecula, CA) and tetramethylrhodamine isothiocyanate (TRITC)-conjugated goat anti-rabbit IgG (1:100, Millipore). After washing, sections were incubated in 0.1% Sudan Black B for 10 min at room temperature and washed with Tx-PBS for 30 min. Sections were coverslipped with Vectashield (Vector Laboratories) and observed with a confocal laser microscope (LSM5 PASCAL; Carl Zeiss MicroImaging gmbh, Jena, Germany).

Immunoblotting

Sarkosyl-insoluble, urea-soluble fractions were extracted from the temporal lobe of an autopsied case with no neurological abnormality as a normal control and cases with AD, DLB and FTLD-U, as previously described [13, 14]. For SDS-PAGE of the samples, 15% polyacrylamide gel was used to visualize low-molecular weight fragments of accumulated

TDP-43 clearly as previously reported [14]. Proteins in the gel were then electrotransferred onto a polyvinylidene difluoride membrane (Millipore Corp., Bedford, MA). After blocking with 3% gelatin in Tris-buffered saline (20 mM Tris–HCl, pH 7.5, 500 mM NaCl), membranes were incubated overnight with pS409/410 or pS403/404. Following incubation with an appropriate biotinylated secondary antibody, labeling was detected using the ABC system coupled with a DAB reaction intensified with nickel chloride.

Results

Immunohistochemical analyses

Accumulation of phosphorylated TDP-43 in AD

As we have described previously, antibodies against pTDP-43 demonstrated abnormal structures only and did not show the diffuse nuclear staining pattern typical of normal TDP-43 [14]. The two primary antibodies (pS409/410 and pS403/404) labeled similar pathological structures with similar sensitivity. pTDP-43-positive structures were present in 36% (19/53) of the first AD series (Tables 1, 3) and in 56% (14/25) of the second AD series (Tables 1, 4) with highly variable severity and regional distribution among these cases. The frequency of pTDP-43 immunoreactivity in the two series was not significantly different ($\chi^2 = 2.826$; 1 *df*; $P = 0.093$). pTDP-43-positive NCIs and DNs were variably present in the amygdala, hippocampus, parahippocampal

Table 3 TDP-43-positive structures in the first series of Alzheimer's disease

Case no.	Age	Sex	SP (CERAD)	NFT (Braak)	Amyg	DG	CA4	CA2/3	CA1	Sub	EC	Temp	TDP-43 path
F-AD1	86	M	NA	NA	+++	NA	NA	NA	NA	++	+++	+++	Diffuse
F-AD2	85	F	C	V	NA	+++	++	++	++	+	+++	+++	Diffuse
F-AD3	80	F	C	V	NA	++	+	+	++	++	+++	+++	Diffuse
F-AD4	67	F	C	VI	NA	±	−	−	+	++	+++	+++	Diffuse
F-AD5	82	M	NA	NA	NA	++	−	±	++	++	++	−	Limbic
F-AD6	85	F	C	VI	NA	+	−	±	±	+	++	−	Limbic
F-AD7	86	M	C	V	+	+	−	−	±	+	++	−	Limbic
F-AD8	86	M	NA	NA	−	−	−	−	±	+	+	−	Limbic
F-AD9	75	M	C	VI	+	+	±	±	±	+	+	±	Limbic
F-AD10	77	M	C	V	NA	NA	NA	NA	NA	++	−	−	Limbic
F-AD11	78	M	C	VI	NA	±	−	−	±	+	−	−	Limbic
F-AD12	96	M	NA	NA	NA	−	−	−	−	+	−	−	Limbic
F-AD13	91	F	C	IV	NA	−	−	−	−	+	−	−	Limbic
F-AD14	89	F	C	V	NA	−	−	−	−	+	−	−	Limbic
F-AD15	81	F	C	V	++	±	−	−	−	+	+	−	Limbic
F-AD16	93	M	C	V	NA	−	−	−	−	+	−	−	Limbic
F-AD17	75	M	C	VI	−	−	−	−	+	+	+	−	Limbic
F-AD18	89	M	C	V	+	−	−	−	−	−	+	−	Limbic
F-AD19	72	F	NA	NA	+	NA	NA	NA	NA	NA	NA	NA	NA

SP Senile plaque, *NFT* neurofibrillary tangle, *Amyg* amygdala, *DG* dentate gyrus, *Sub* subiculum, *EC* entorhinal cortex, *Temp* temporal cortex, *path* pathology, *NA* not available

−, None; ±, slight; +, mild; ++, moderate; +++, severe

**Table 4** TDP-43-positive structures in the second series of Alzheimer's disease

Case no.	Age	Sex	SP (CERAD)	NFT (Braak)	Amyg	DG	CA4	CA2/3	CA1	Sub	EC	Cing	Temp	Front	Par	TDP-43 path
S-AD1	72	F	C	VI	+++	++	+	+	+++	+++	+++	+	+++	+	−	Diffuse
S-AD2	85	M	C	V	+++	+++	+++	+++	+++	+++	+++	+++	+++	++	+	Diffuse
S-AD3	84	M	C	V	+++	+++	+	++	++	+++	+++	++	+++	+++	+	Diffuse
S-AD4	89	M	C	VI	+++	++	±	+	+++	+++	+++	+	++	−	−	Diffuse
S-AD5	81	F	C	VI	+++	++	−	±	+++	+++	+++	+	++	−	−	Diffuse
S-AD6	80	M	C	VI	+++	+	±	+	+++	++	++	±	−	−	−	Limbic
S-AD7	80	F	C	VI	++	±	−	−	++	++	++	−	−	−	−	Limbic
S-AD8	89	F	C	VI	±	+	±	+	+++	+++	+	−	−	−	−	Limbic
S-AD9	84	F	C	VI	++	−	−	−	±	+	+	−	−	−	−	Limbic
S-AD10	95	M	C	VI	++	−	−	−	±	±	+	−	−	−	−	Limbic
S-AD11	74	F	C	VI	±	−	−	−	−	−	−	−	−	−	−	Amygdala
S-AD12	72	M	C	VI	±	−	−	−	−	−	−	−	−	−	−	Amygdala
S-AD13	79	M	C	VI	+	−	−	−	−	−	−	−	−	−	−	Amygdala
S-AD14	73	M	C	VI	±	−	−	−	−	−	−	−	−	−	−	Amygdala

SP Senile plaque, *NFT* neurofibrillary tangle, *Amyg* amygdala, *DG* dentate gyrus, *Sub* subiculum, *EC* entorhinal cortex, *Cing* cingulate cortex, *Temp* temporal cortex, *Front* frontal cortex, *Par* parietal cortex, *path* pathology

−, None; ±, slight; +, mild; ++, moderate; +++, severe

gyrus and neocortex (Fig. 1). In cases where the neocortex was involved, NCIs and DNs were predominantly distributed in the upper layers, most closely resembling FTLD-U type 3. Moreover, most of these cases also had a few NIIs with a lentiform shape in the dentate gyrus or the neocortex, similar to those characteristic of cases with *PGRN* mutations [26] (Fig. 1k, inset). Neurofibrillary tangle-like pTDP-43-positive structures were occasionally found in the CA1 region (Fig. 1f). Small round, short thread-like or coiled body-like structures were sometimes observed in the white
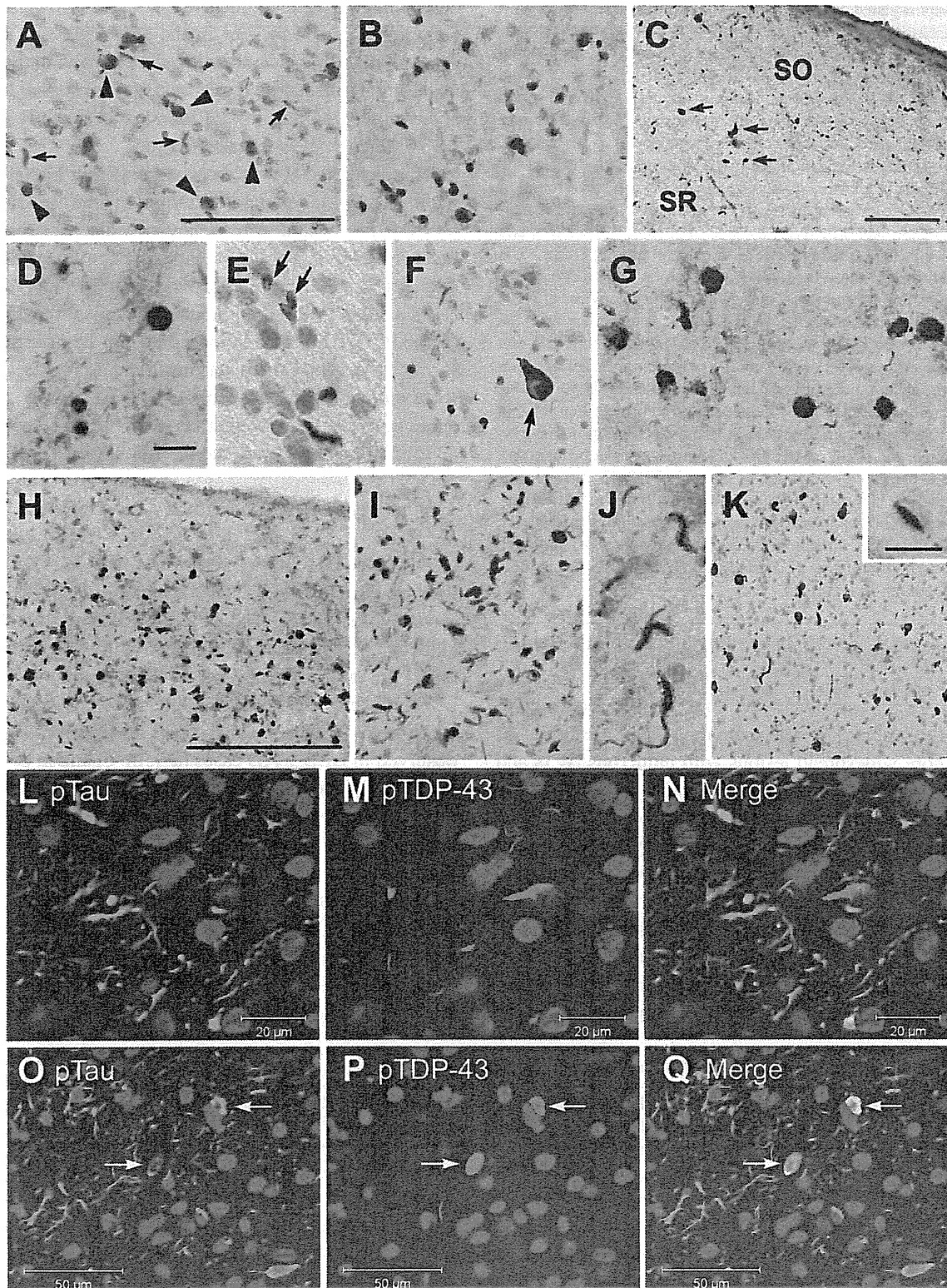
matter, including the stratum radiatum and the stratum oriens of the CA2/3 region, alveus and parahippocampal white matter. In double labeling immunofluorescence experiments, cortical tau-positive neuropil threads and TDP-43-positive dystrophic neurites were usually stained independently (Fig. 1l–n), while some neurons showed cytoplasmic inclusions immunoreactive for both markers (Fig. 1o–q).

In 19 cases with pTDP-43 immunoreactivity in the first series (Table 3), pTDP-43 pathology was largely restricted

◀ **Fig. 1** Phosphorylated TDP-43 (*pTDP-43*) positive structures in Alzheimer's disease cases with diffuse type of TDP-43 pathology. **a** Neuronal cytoplasmic inclusions (NCIs) (*arrowheads*) and dystrophic neurites (DNs) (*arrows*) in amygdala. **b** NCIs in the granule cells of the dentate gyrus. **c** NCIs in the principal layer (*arrows*) and small round or short threads-like structures in the stratum oriens (*SO*) and stratum radiatum (*SR*) of the CA2/3 region. **d** A high power view of small round or short threads-like structures in the stratum oriens of the CA2/3 region. **e** Glial cytoplasmic inclusions (*arrows*) and a small round or a short threads-like structure in the alveus of the CA1 region. **f** A neurofibrillary tangle-like structure (*arrow*), small round structures and short neurites in the principal layer of the CA1 region. **g** Large NCIs and short neurites in the subiculum. **h** Massive NCIs and DNs in the superficial layer of the entorhinal cortex. **i** A high power view of NCIs and DNs in the entorhinal cortex. **j** Glial cytoplasmic inclusions in the white matter of the parahippocampal gyrus. **k** Numerous NCIs and DNs in the superficial layer of the lateral occipitotemporal cortex. *Inset* shows a neuronal intranuclear inclusion with a lentiform shape. Double label immunofluorescence (**l–q**) demonstrates that most tau-positive neuropil threads (*green fluorescence* in **l**) and pTDP-43 positive DNs (*red fluorescence* in **m**) in the temporal neocortex are independent (**n**), while there is partial colocalization of tau and pTDP-43 in some neuronal cytoplasmic inclusions (*arrows* in **o–q**). Immunohistochemistry using primary antibodies pS403/404 (**a, e, f, k**) and pS409/410 (**b, c, d, g, h, i, j**). Double label immunofluorescence with anti-phosphorylated tau (AT8) and pS403/404 (**l–q**). *Scale bars* **a, b, c, f, g, i** 100 μm; **d, e, j**, *inset* in **k** 10 μm; **h, k** 200 μm

to the limbic region (amygdala, hippocampus and entorhinal cortex) in 14 cases (73.7%). This distribution of pTDP-43 pathology corresponds to the "limbic type" according to Amador-Ortiz et al. [1]. The remaining four cases (21.1%) showed more widespread lesions with numerous NCIs and DNs in the temporal neocortex; corresponding to the "diffuse type" according to Amador-Ortiz et al. [1]. Of the 14 cases with pTDP-43 immunoreactivity in the second series (Table 4), pTDP-43 pathology was found only in the amygdala in 4 cases (28.6%), showed more widespread involvement of limbic structures in 5 cases (35.7%) and extended into the cerebral neocortex in the remaining 5 cases (35.7%).There appeared to be a hierarchy to the anatomical distribution and severity of involvement that was best demonstrated in the second series (Table 4). The pathology seemed to start in the amygdala and then progress to other limbic structures before involving the neocortex. Among neocortical regions, the temporal lobe was always involved, the frontal lobe less frequently and only rarely the parietal lobe was affected.

The mean age at death was significantly higher in cases with pTDP-43 immunoreactivity in the second series ($P = 0.015$). A similar tendency was also observed in the first series, but it was not statistically significant ($P = 0.16$). The Braak NFT stage score was significantly higher in cases with pTDP-43 immunoreactivity in the first series ($P = 0.027$). This correlation could not be assessed in the second series since there was insufficient range in the Braak stage among the cases (Tables 1, 4). There were no differences in sex or brain weight between the cases with pTDP-43 immunoreactivity and those without (see Table 1).

Accumulation of phosphorylated TDP-43 in DLB

pTDP-43-positive structures were found in 53% (7/15) of the first DLB series (Tables 1, 5) and in 60% (6/10) of the second DLB series (Tables 1, 6) with variable frequency and regional distribution. There was no significant difference in the frequency of pTDP-43 immunoreactivity between the two series ($\chi^2 = 0.000$; 1 *df*; $P > 0.999$).

Figure 2 illustrates pTDP-43-positive structures observed in DLB + AD cases (a–j, m–o) and in pure DLBD cases (k, l). The morphology and anatomical distribution of the pathology was similar to that seen in the series of AD cases and the neocortical involvement again resembled FTLD-U Type 3 with a few lentiform NIIs. In double labeling confocal microscopy for pTDP-43 and phosphorylated α-synuclein in the cortex, some neurons showed cytoplasmic inclusions immunoreactive for both markers (m–o).

Of the eight cases with pTDP-43 immunoreactivity in the first DLB series (Table 5), TDP-43 pathology was

Table 5 TDP-43-positive structures in the first series of dementia with Lewy bodies

Case no.	Age	Sex	SP (CERAD)	NFT (Braak)	DLB likelihood	Pathological diagnosis	Amyg	DG	CA4	CA2/3	CA1	Sub	EC	Temp	TDP-43 path
F-DLB1	63	F	C	VI	Int.	DLB + AD	NA	+++	+	++	+	++	+++	++	Diffuse
F-DLB2	67	M	C	VI	Int.	DLB + AD	+++	+++	+	++	+	++	+++	++	Diffuse
F-DLB3	82	F	C	VI	Int.	DLB + AD	NA	+	±	+	+	++	++	+	Diffuse
F-DLB4	83	M	C	IV	High	DLB + AD	+++	+	−	+	+	++	+++	−	Limbic
F-DLB5	89	M	C	IV	High	DLB + AD	NA	−	−	+	−	+	+	−	Limbic
F-DLB6	71	M	C	IV	High	DLB + AD	NA	±	−	±	−	±	±	−	Limbic
F-DLB7	51	M	0	II	High	DLB	++	+	+	++	±	++	++	−	Limbic
F-DLB8	82	M	0	II	High	DLB	+	−	−	−	−	−	+	−	Limbic

SP Senile plaque, *NFT* neurofibrillary tangle, *Amyg* amygdala, *DG* dentate gyrus, *Sub* subiculum, *EC* entorhinal cortex, *Temp* temporal cortex, *path* pathology, *NA* not available

−, None; ±, slight; +, mild; ++, moderate; +++, severe

🖄 Springer

Table 6 TDP-43-positive structures in the second series of dementia with Lewy bodies

Case no.	Age	Sex	SP (CERAD)	NFT (Braak)	DLB likelihood	Pathological diagnosis	Amyg	DG	CA4	CA2/3	CA1	Sub	EC	Cing	Temp	Front	Par	TDP-43 path
S-DLB1	90	F	C	VI	Int.	DLB + AD	+++	−	−	−	−	+	±	−	−	−	−	Limbic
S-DLB2	79	M	C	VI	Int.	DLB + AD	++	−	−	−	−	−	±	−	−	−	−	Limbic
S-DLB3	74	M	0	II	High	DLB	+	−	−	−	−	−	−	−	−	−	−	Amygdala
S-DLB4	70	M	C	II	High	DLB	+	NA	NA	NA	NA	NA	NA	−	−	−	−	Amygdala
S-DLB5	71	M	C	III	High	DLB	±	−	−	−	−	−	−	−	−	−	−	Amygdala
S-DLB6	74	F	C	VI	Int.	DLB + AD	±	−	−	−	−	−	−	−	−	−	−	Amygdala

SP Senile plaque, *NFT* neurofibrillary tangle, *Amyg* amygdala, *DG* dentate gyrus, *Sub* subiculum, *EC* entorhinal cortex, *Cing* cingulate cortex, *Temp* temporal cortex, *Front* frontal cortex, *Par* parietal cortex, *path* pathology, *NA* not available

−, None; ±, slight; +, mild; ++, moderate; +++, severe

largely confined to limbic region in five cases (62.5%), while three cases (37.5%) revealed more widespread lesions in the temporal cortex. In the second series (Table 6), four cases (66.7%) showed slight TDP-43 pathology only in amygdala and the remaining two cases (33.3%) showed moderate to severe TDP-43 pathology in amygdala and slight to mild TDP-43 pathology in limbic region.

There were no significant differences in the mean age at death, sex and Braak NFT stage score between cases with pTDP-43 immunoreactivity and those without, in either series (see Table 1). All three cases with pure DLB had some TDP-43 pathology.

Biochemical analyses of accumulated TDP-43 in AD and DLB

Figure 3 shows immunoblot analyses of sarkosyl-insoluble, urea-soluble fractions extracted from brains of a normal control (lane 1), AD without pTDP-43 immunoreactivity (AD−, lane 2), DLB with pTDP-43 immunoreactivity (DLB+, F-DLB2, see Table 5) (lane 3), AD with pDP-43 immunoreactivity (AD+, F-AD1, see Table 3) (lane 4), FTLD-U, Type 3 (lane 5), and FTLD-U, Type 1 (lane 6). With phosphorylation-dependent antibodies specific for pS409/410 (a) and for pS403/404 (b), intense immunoreactivity throughout the gel was observed only in DLB+ (lane 3), AD+ (lane 4), FTLD-U, Type 3 (lane 5), and FTLD-U, Type 1 (lane 6). Regarding low-molecular-weight fragments, DLB+ (lane 3) and AD+ (lane 4) showed a similar pattern with three major bands at 23, 24 and 26 kDa and two minor bands at 18 and 19 kDa. Of three major bands, a 23 kDa band was the most intense, while the immunoreactivity of two minor bands at 18 and 19 kDa was similar. This band pattern corresponds to that of FTLD-U, Type 3 (see lane 5 in a, b and schematic diagram in c), previously reported by us [14]. FTLD-U with Type 1 (lane 6) showed a band pattern with two major bands at 23 and 24 kDa and

two minor bands at 18 and 19 kDa, which is consistent with our previous report [14].

Discussion

In this study, we used phosphorylation-dependent anti-TDP-43 antibodies to perform detailed immunohistochemical and biochemical examination of two independent series of brains with AD and DLB. We found higher frequencies of TDP-43 pathology in AD (36–56%) and DLB (53–60%) than in previous reports [1, 16, 17, 19, 28, 36]. This may be due to the two immunohistochemical protocols we employed, one on free-floating sections and the other using an automated immunostainer for paraffin sections, are more sensitive than the methods used in previous studies. In addition, the higher frequencies found in our second series are partially explained by inclusion of examination of the amygdala, the region that appears to be most often affected by TDP-43 pathology [17].

The largely consistent observations between our two series, despite differences in the ethnic populations and source of the clinical cases, suggest that our findings are more likely to be broadly applicable to other populations of AD and DLB patients. We have also demonstrated that similar findings are attainable using various immunohistochemical methodology employed by different labs.

In immunohistochemical examinations of AD and DLB cases in the present study, phosphorylation-dependent anti-TDP-43 antibodies stained NCIs and DNs in the cerebral grey matter as previously reported [1, 16, 30, 39], and some thread-like or coiled body-like structures in the whiter matter. Regarding the distribution of TDP-43 pathology in AD, Amador-Ortiz et al. [1] first classified it into limbic and diffuse types, and indicated that limbic involvement was more common. Subsequently, Hu et al. [17] found some AD cases with TDP-43 pathology confined to the amygdala only. They suggested that the amygdala is the most susceptible
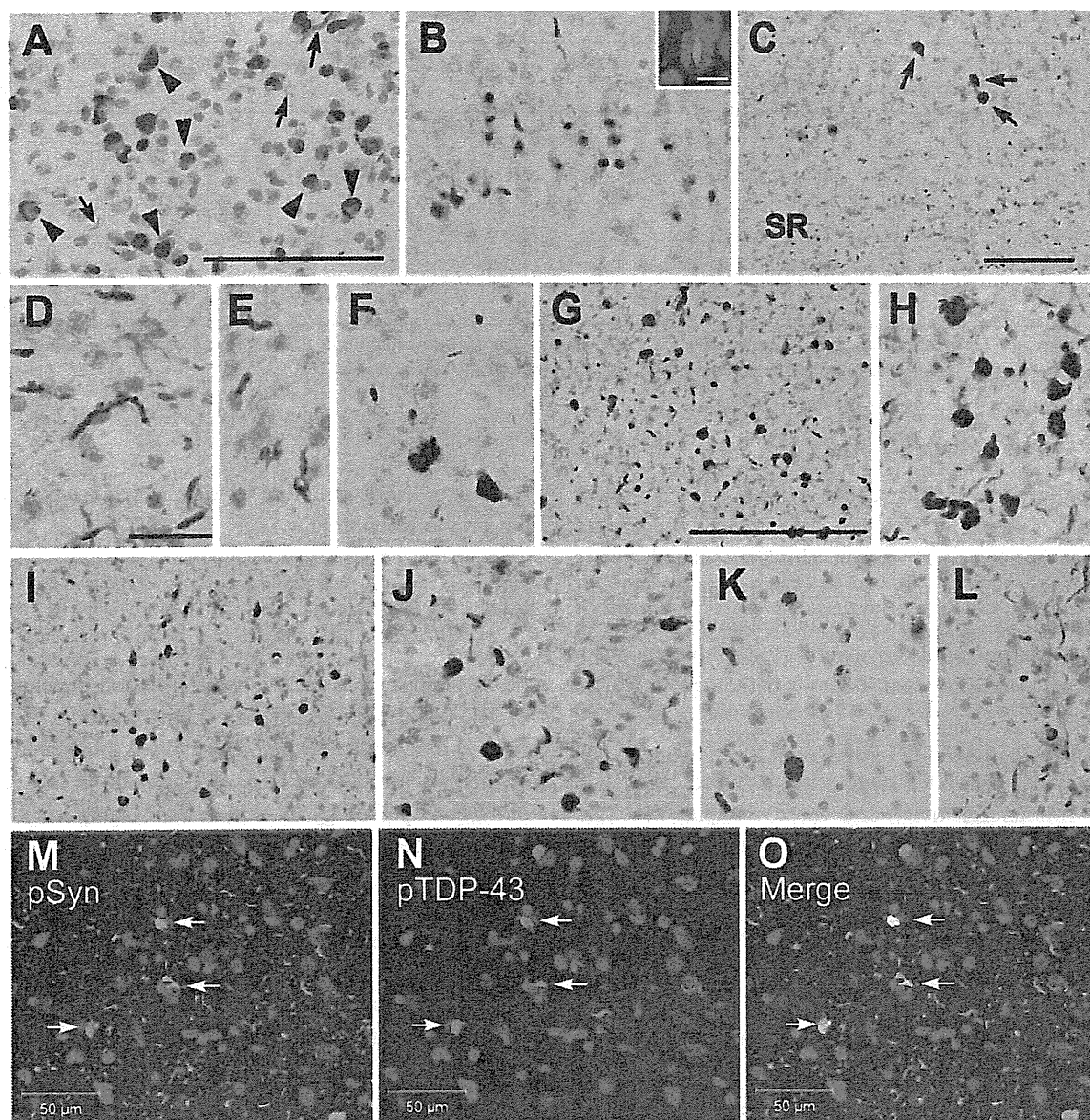
Fig. 2 Phosphorylated TDP-43 (*pTDP-43*) positive structures in cases of dementia with Lewy bodies. TDP-43 positive structures in cases of DLB plus AD with diffuse type of TDP-43 pathology are shown in **a**–**j**. Neuronal cytoplasmic inclusions (NCIs) and dystrophic neurites (DNs) in the entorhinal cortex of the pure DLB cases without AD pathology are shown in **k** (F-DLB7) and **l** (F-DLB8). **a** NCIs (*arrowheads*) and DNs (*arrows*) in amygdala. **b** NCIs in the dentate granule cells. *Inset* shows immunofluorescence staining of a lentiform inclusion (*red*) in the nucleus (*blue*) of a granule cell. **c** NCIs in the principal layer (*arrows*) and massive short threads-like structures in the stratum radiatum (*SR*) of the CA2/3 region. **d** A high power view of short threads-like structures in the stratum radiatum of the CA2/3 region. **e** Short threads-like structure in the alveus of the CA1 region. **f** Large region, and that TDP-43 pathology in AD spreads from limbic structures to association cortices. In the present study, we observed amygdala only, limbic, and diffuse patterns of pTDP-43 pathology, not only in AD cases but also in DLB cases. These results suggest a common progressive NCIs and short neurites in the subiculum. **g** Massive NCIs and DNs in the superficial layer of the entorhinal cortex. **h** A high power view of NCIs and DNs in the entorhinal cortex. **i** Numerous NCIs and DNs in the superficial layer of the lateral occipitotemporal cortex. **j** A high power view of NCIs and DNs in the lateral occipitotemporal cortex. Double label immunofluorescence (**m**–**o**) shows partial co-localization of α-synuclein and pTDP-43 in the NCIs in the temporal neocortex (*arrows*), whereas most α-synuclein-positive neurites are negative for pTDP-43 (**m**–**o**). Immunostaining with pS403/404 (**a**, **i**, **j**) and pS409/410 (**b**–**h**, **k**, **l**). Double label immunofluorescence with anti-phosphorylated α-synuclein (pα#64) and pS403/404 (**m**–**o**). *Scale bars* **a**, **b**, **f**, **h**, **j**–**l** 100 μm; **d**, **e** 25 μm; **c**, **g**, **i** 200 μm; *inset* in **b** 10 μm

anatomical pattern of pTDP-43 pathology in AD and DLB, with sequential spread from the amygdala to other limbic structures and then to association cortices. Although the number of cases was small, the results from our second series also suggests that there may be hierarchical involvement
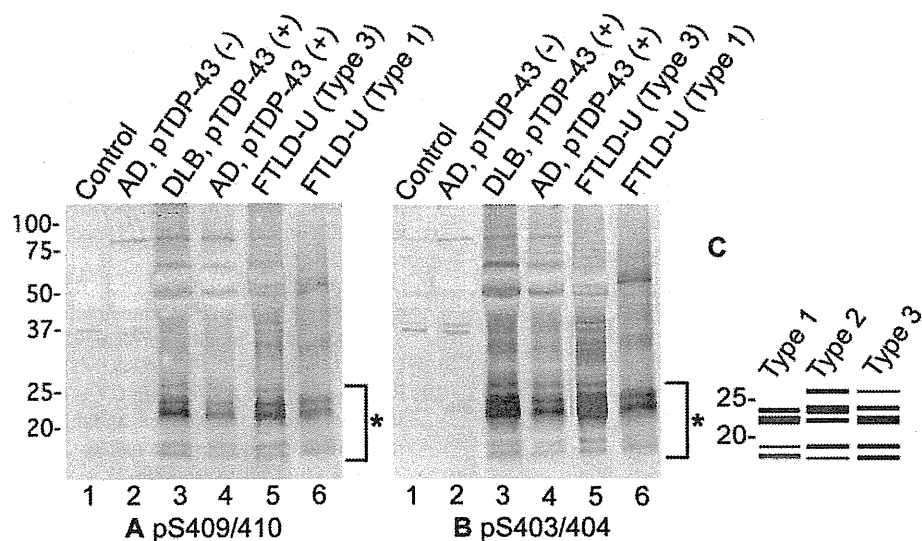
Fig. 3 The band pattern of the C-terminal fragments of phosphory-lated TDP-43 (*pTDP-43*) in Alzheimer's disease (*AD*) and dementia with Lewy bodies (*DLB*). Immunoblot analyses of sarkosyl-insoluble, urea-soluble fractions, using phosphorylation-dependent anti-TDP-43 antibodies pS409/410 (a) and pS403/404 (b). *Lane 1* normal control; *lane 2* AD without pTDP-43 immunoreactivity (AD–); *lane 3* DLB with pTDP-43 immunoreactivity (DLB+); *lane 4* AD with pTDP-43 immunoreactivity (AD+); *lane 5* FTLD-U with Type 3 TDP-43 pathol-ogy; *lane 6* FTLD-U with Type 1 TDP-43 pathology. Schematic dia-gram (c) showing the band pattern of the C-terminal fragments of phosphorylated TDP-43 we have previously reported [14]. Strong immunoreactivity throughout the gel is observed only in DLB+ (*lane 3*), AD+ (*lane 4*) and FTLD-U (*lanes 5, 6*). DLB+ (*lane 3*), AD+ (*lane 4*) and FTLD-U, Type 3 (*lane 5*) show similar patterns of low M_r bands with three major bands at 23, 24 and 26 kDa and two minor bands at 18 and 19 kDa, while FTLD-U, Type 1 (*lane 6*) shows two major bands at 23 and 24 kDa and two minor bands at 18 and 19 kDa (*asterisk*)

of neocortical regions, with the temporal association cortex involved first, followed by the frontal lobe and parietal lobe last.

Since subclassification of FTLD-U is based on TDP-43 pathology in the neocortex [7, 25, 35], only AD and DLB cases with the diffuse type of TDP-43 pathology could be subtyped. All of these cases had pTDP-43-positive NCIs and short DNs in the upper cortical layers, which corre-sponds to FTLD-U Type 3. In addition, most of them (8 of 9 AD cases and 2 of 3 DLB cases with the diffuse type) also had a few pTDP-43-positive NIIs in the dentate gyrus or the neocortex, These findings are consistent with the previous reports by Uryu et al. [39] and Nakashima-Yasuda et al. [30], but differ somewhat from Joseph et al. [19] who reported all three FTLD-U subtypes in AD, with the major-ity being Type 2.

Perhaps the greatest significance of this study is the evi-dence it provides that the pathological TDP-43 that accu-mulates in AD and DLB is similar to that in FTLD-U. First, positive staining of abnormal structures in immunohisto-chemistry and of abnormal bands on immunoblots of sarko-syl-insoluble fraction with pS403/404 and pS409/410 antibodies suggest that C-terminal phosphorylation sites of TDP-43 accumulated in AD and DLB brains are common to those in FTLD-U brains [14]. Second, intense staining of low-molecular-weight bands around 20–25 kDa on immu-noblotting of sarkosyl-insoluble fraction from AD and DLB cases with neocortical pTDP-43 pathology indicates that

the generation of C-terminal fragments of TDP-43 takes place in brains of these diseases as it does in FTLD-U [14, 18]. Furthermore, the band pattern of C-terminal fragments in AD and DLB corresponds to that of FTLD-U, Type 3, found in our previous report [14]. These findings suggest that there may be a common process that leads to the accu-mulation of pathological TDP-43 in FTLD-U Type 3, and some cases of AD and DLB. In this context, it should be noted that cases of familial FTLD-U with *PGRN* mutations always show Type 3 TDP-43 pathology [7]. Some familial FTLD-U cases with *PGRN* mutations have additional AD pathology [29] or tau and α-synuclein pathology [22]. Sev-eral mutations and polymorphisms of *PGRN* have recently been identified in AD and Parkinson's disease populations [5, 6] and these might underlie the co-occurrence of abnor-mal deposition of TDP-43, tau, and α-synuclein. Further-more, a common genetic variant in *PGRN* (rs5848), located within a binding site for miR-659, has recently been identi-fied as a major susceptibility factor for sporadic FTLD-U [34]. Homozygosity for the T-allele of rs5848 causes a sig-nificant reduction in the level of PGRN protein and is asso-ciated with a 3.2-fold increased risk of developing FTLD-U. The majority of these cases have Type 3 TDP-43 pathol-ogy. It is therefore possible that the subset of AD and DLB patients who develop TDP-43 pathology are carriers of this, or some other genetic risk factor, for TDP-43 proteinopa-thy. Partial colocalization of tau and TDP-43 or α-synuclein and TDP-43 in some cytoplasmic inclusions found in this

and other studies [1, 11, 13, 16, 30] may argue against a direct interaction between these proteins, and support the notion that there may be genetic or environmental factors that make the subset of neurons vulnerable for intracellular accumulation of tau, α-synuclein and TDP-43.

The fact that the accumulated TDP-43 in AD and DLB is biochemically similar to that believed to be pathogenic in FTLD-U, suggests that it might contribute to neurodegeneration or modify the clinical course. At present, there is a little data regarding the relationship between the presence of TDP-43 pathology and the clinical phenotype of AD or DLB. The older age at death of the AD cases with pTDP-43 pathology, observed in our second series (Table 4), is consistent with the previous report by Joseph et al. [19]. Nakashima-Yasuda et al. [30] also found a higher average age at death in the TDP-43 positive cases in Lewy body related diseases with dementia. A higher Braak NFT stage in the TDP-43 positive patients was found in DLB + AD cases by Nakashima-Yasuda et al. [30] and also in our first series of AD (Table 1). Further studies using larger cohorts with more detailed clinical, radiological and pathological data are needed to elucidate the clinical impact of TDP-43 pathology in AD and DLB.

References

1. Amador-Ortiz C, Lin WL, Ahmed Z et al (2007) TDP-43 immunoreactivity in hippocampal sclerosis and Alzheimer's disease. Ann Neurol 61:435–445. doi:10.1002/ana.21154
2. Arai T, Hasegawa M, Akiyama H et al (2006) TDP-43 is a component of ubiquitin-positive tau-negative inclusions in frontotemporal lobar degeneration and amyotrophic lateral sclerosis. Biochem Biophys Res Commun 351:602–611. doi:10.1016/j.bbrc.2006.10.093
3. Arai T, Ikeda K, Akiyama H et al (2003) Different immunoreactivities of the microtubule-binding region of tau and its molecular basis in brains from patients with Alzheimer's disease, Pick's disease, progressive supranuclear palsy and corticobasal degeneration. Acta Neuropathol 105:489–498
4. Baker M, Mackenzie IR, Pickering-Brown SM et al (2006) Mutations in progranulin cause tau-negative frontotemporal dementia linked to chromosome 17. Nature 442:916–919. doi:10.1038/nature05016
5. Brouwers N, Nuytemans K, van der Zee J et al (2007) Alzheimer and Parkinson diagnoses in progranulin null mutation carriers in an extended founder family. Arch Neurol 64:1436–1446. doi:10.1001/archneur.64.10.1436
6. Brouwers N, Sleegers K, Engelborghs S et al (2008) Genetic variability in progranulin contributes to risk for clinically diagnosed Alzheimer disease. Neurology 71:656–664. doi:10.1212/01.wnl.0000319688.89790.7a
7. Cairns NJ, Neumann M, Bigio EH et al (2007) TDP-43 in familial and sporadic frontotemporal lobar degeneration with ubiquitin inclusions. Am J Pathol 171:227–240. doi:10.2353/ajpath.2007.070182
8. Cruts M, Gijselinck I, van der Zee J et al (2006) Null mutations in progranulin cause ubiquitin-positive frontotemporal dementia linked to chromosome 17q21. Nature 442:920–924. doi:10.1038/nature05017
9. Davidson Y, Kelley T, Mackenzie IRA et al (2007) Ubiquitinated pathological lesions in frontotemporal lobar degeneration contain the TAR DNA-binding protein, TDP-43. Acta Neuropathol 113:521–533. doi:10.1007/s00401-006-0189-y
10. Feldman H, Levy AR, Hsiung GY et al (2003) A Canadian cohort study of cognitive impairment and related dementias (ACCORD): study methods and baseline results. Neuroepidemiology 22:265–274. doi:10.1159/000071189
11. Freeman SH, Spires-Jones T, Hyman BT, Growdon JH, Frosch MP (2008) TAR-DNA binding protein 43 in Pick disease. J Neuropathol Exp Neurol 67:62–67. doi:10.1097/nen.0b013e3181609361
12. Gitcho MA, Baloh RH, Chakraverty S et al (2008) TDP-43 A315T mutation in familial motor neuron disease. Ann Neurol 63:535–538. doi:10.1002/ana.21344
13. Hasegawa M, Arai T, Akiyama H et al (2007) TDP-43 is deposited in the Guam parkinsonism–dementia complex brains. Brain 130:1386–1394. doi:10.1093/brain/awm065
14. Hasegawa M, Arai T, Nonaka T et al (2008) Phosphorylated TDP-43 in frontotemporal lobar degeneration and amyotrophic lateral sclerosis. Ann Neurol 64:60–70. doi:10.1002/ana.21425
15. Higashi S, Iseki E, Yamamoto R et al (2007) Appearance pattern of TDP-43 in Japanese frontotemporal lobar degeneration with ubiquitin-positive inclusions. Neurosci Lett 419:213–218. doi:10.1016/j.neulet.2007.04.051
16. Higashi S, Iseki E, Yamamoto R et al (2007) Concurrence of TDP-43, tau and alpha-synuclein pathology in brains of Alzheimer's disease and dementia with Lewy bodies. Brain Res 1184:284–294. doi:10.1016/j.brainres.2007.09.048
17. Hu WT, Josephs KA, Knopman DS et al (2008) Temporal lobar predominance of TDP-43 neuronal cytoplasmic inclusions in Alzheimer disease. Acta Neuropathol 116:215–220. doi:10.1007/s00401-008-0400-4
18. Igaz LM, Kwong LK, Xu Y et al (2008) Enrichment of C-terminal fragments in TAR DNA-binding protein-43 cytoplasmic inclusions in brain but not in spinal cord of frontotemporal lobar degeneration and amyotrophic lateral sclerosis. Am J Pathol 173:182–194. doi:10.2353/ajpath.2008.080003
19. Josephs KA, Whitwell JL, Knopman DS et al (2008) Abnormal TDP-43 immunoreactivity in AD modifies clinicopathologic and radiologic phenotype. Neurology 70:1850–1857. doi:10.1212/01.wnl.0000304041.09418.b1
20. Kabashi E, Valdmanis PN, Dion P et al (2008) TARDBP mutations in individuals with sporadic and familial amyotrophic lateral sclerosis. Nat Genet 40:572–574. doi:10.1038/ng.132
21. Kosaka K (1990) Diffuse Lewy body disease in Japan. J Neurol 237:197–204. doi:10.1007/BF00314594
22. Leverenz JB, Yu CE, Montine TJ et al (2007) A novel progranulin mutation associated with variable clinical presentation and tau, TDP43 and alpha-synuclein pathology. Brain 130:1360–1374. doi:10.1093/brain/awm069
23. Lin WL, Dickson DW (2008) Ultrastructural localization of TDP-43 in filamentous neuronal inclusions in various neurodegenerative diseases. Acta Neuropathol 116:205–213. doi:10.1007/s00401-008-0408-9
24. Mackenzie IR, Bigio EH, Ince PG et al (2007) Pathological TDP-43 distinguishes sporadic amyotrophic lateral sclerosis from

amyotrophic lateral sclerosis with SOD1 mutations. Ann Neurol 61:427–434. doi:10.1002/ana.21147

25. Mackenzie IRA, Baborie A, Pickering-Brown S et al (2006) Heterogeneity of ubiquitin pathology in frontotemporal lobar degeneration: classification and relation to clinical phenotype. Acta Neuropathol 112:539–549. doi:10.1007/s00401-006-0138-9

26. Mackenzie IRA, Baker M, Pickering-Brown S et al (2006) The neuropathology of frontotemporal lobar degeneration caused by mutations in the progranulin gene. Brain 129:3081–3090. doi:10.1093/brain/awl271

27. McKeith IG, Dickson DW, Lowe J et al (2005) Diagnosis and management of dementia with Lewy bodies: third report of the DLB Consortium. Neurology 65:1863–1872. doi:10.1212/01.wnl. 0000187889.17253.b1

28. Morita M, Al-Chalabi A, Anderson PM et al (2006) A locus on chromosome 9p confers susceptibility to ALS and frontotemporal dementia. Neurology 66:839–844. doi:10.1212/01.wnl. 0000200048.53766.b4

29. Mukherjee O, Pastor P, Cairns NJ et al (2006) HDDD2 is a familial frontotemporal lobar degeneration with ubiquitin-positive tau-negative inclusions caused by a missense mutation in the signal peptide of progranulin. Ann Neurol 60:314–322. doi:10.1002/ana. 20963

30. Nakashima-Yasuda H, Uryu K, Robinson J et al (2007) Co-morbidity of TDP-43 proteinopathy in Lewy body related diseases. Acta Neuropathol 114:221–229. doi:10.1007/s00401-007-0261-2

31. Neumann M, Kwong LK, Sampathu DM, Trojanowski JQ, Lee VM (2007) TDP-43 proteinopathy in frontotemporal lobar degeneration and amyotrophic lateral sclerosis: protein misfolding diseases without amyloidosis. Arch Neurol 64:1388–1394. doi:10.1001/archneur.64.10.1388

32. Neumann M, Sampathu DM, Kwong LK et al (2006) Ubiquitinated TDP-43 in frontotemporal lobar degeneration and amyotrophic lateral sclerosis. Science 314:130–133. doi:10.1126/science. 1134108

33. Newell KL, Hyman BT, Growdon JH, Hedley-Whyte ET (1999) Application of the National Institute on Aging (NIA)–Reagan Institute criteria for the neuropathological diagnosis of Alzheimer disease. J Neuropathol Exp Neurol 58:1147–1155. doi:10.1097/ 00005072-199911000-00004

34. Rademakers R, Eriksen JL, Baker M et al (2008) Common variation in the miR-659 binding-site of GRN is a major risk factor for TDP43-positive frontotemporal dementia. Hum Mol Genet 17:3631–3642. doi:10.1093/hmg/ddn257

35. Sampathu DM, Neumann M, Kwong LK et al (2006) Pathological heterogeneity of frontotemporal lobar degeneration with ubiquitin-positive inclusions delineated by ubiquitin immunohistochemistry and novel monoclonal antibodies. Am J Pathol 169:1343–1352. doi:10.2353/ajpath.2006.060438

36. Schwab C, Arai T, Hasegawa M, Yu S, McGeer PL (2008) Colocalization of transactivation-responsive DNA-binding protein 43 and huntingtin in inclusions of Huntington disease. J Neuropathol Exp Neurol 67(12):1159–1165

37. Sreedharan J, Blair IP, Tripathi VB et al (2008) TDP-43 mutations in familial and sporadic amyotrophic lateral sclerosis. Science 319:1668–1672. doi:10.1126/science.1154584

38. Tan CF, Eguchi H, Tagawa A et al (2007) TDP-43 immunoreactivity in neuronal inclusions in familial amyotrophic lateral sclerosis with or without SOD1 gene mutation. Acta Neuropathol 113:535–542. doi:10.1007/s00401-007-0206-9

39. Uryu K, Nakashima-Yasuda H, Forman MS et al (2008) Concomitant TAR-DNA-binding protein 43 pathology is present in Alzheimer disease and corticobasal degeneration but not in other tauopathies. J Neuropathol Exp Neurol 67:555–564. doi:10.1097/ NEN.0b013e31817713b5

40. Van Deerlin VM, Leverenz JB, Bekris LM et al (2008) TARDBP mutations in amyotrophic lateral sclerosis with TDP-43 neuropathology: a genetic and histopathological analysis. Lancet Neurol 7:409–416. doi:10.1016/S1474-4422(08)70071-1

41. Vance C, Al-Chalabi A, Ruddy D et al (2006) Familial amyotrophic lateral sclerosis with frontotemporal dementia is linked to a locus on chromosome 9p13.2–21.3. Brain 129:868–875. doi:10.1093/brain/ awl030

42. Watts GDJ, Wymer J, Kovach MJ et al (2004) Inclusion body myopathy associated with Paget disease of bone and frontotemporal dementia is caused by mutant valosin-containing protein. Nat Genet 36:377–381. doi:10.1038/ng1332

43. Yokoseki A, Shiga A, Tan CF et al (2008) TDP-43 mutation in familial amyotrophic lateral sclerosis. Ann Neurol 63:538–542. doi:10.1002/ana.21392

Post mortem cerebrospinal fluid α-synuclein levels are raised in multiple system atrophy and distinguish this from the other α-synucleinopathies, Parkinson's disease and Dementia with Lewy bodies

P.G. Foulds [a], O. Yokota [b,c], A. Thurston [b], Y. Davidson [b], Z. Ahmed [d], J. Holton [d], J.C. Thompson [e], H. Akiyama [f], T. Arai [f], M. Hasegawa [g], A. Gerhard [b], D. Allsop [a,*], D.M.A. Mann [b]

[a] Division of Biomedical and Life Sciences, Faculty of Health and Medicine, University of Lancaster, Lancaster, LA1 4AY, UK
[b] Neurodegeneration and Mental Health Research Group, School of Community Based Medicine, University of Manchester, Hope Hospital, Salford, M6 8HD, UK
[c] Department of Neuropsychiatry, Okayama University Graduate School of Medicine, Dentistry and Pharmaceutical Sciences, 2-5-1 Shikata-cho, Okayama, 700–8558, Japan
[d] Department of Molecular Neuroscience, Institute of Neurology, University College London, Queen Square, WC1N 3BG, London
[e] Cerebral Function Unit, Salford Royal Hospitals NHS Foundation Trust, Hope Hospital, Stott Lane, Salford, M6 8HD, UK
[f] Department of Psychogeriatrics, Tokyo Institute of Psychiatry, 2-1-8 Kamikitazawa, Setagaya-ku, Tokyo, 156–8585, Japan
[g] Department of Molecular Neurobiology, Tokyo Institute of Psychiatry, 2-1-8 Kamikitazawa, Setagaya-ku, Tokyo, 156–8585, Japan

ARTICLE INFO

ABSTRACT

Differentiating clinically between Parkinson's disease (PD) and the atypical parkinsonian syndromes of Progressive supranuclear palsy (PSP), corticobasal syndrome (CBS) and multiple system atrophy (MSA) is challenging but crucial for patient management and recruitment into clinical trials. Because PD (and the related disorder Dementia with Lewy bodies (DLB)) and MSA are characterised by the deposition of aggregated forms of α-synuclein protein (α-syn) in the brain, whereas CBS and PSP are tauopathies, we have developed immunoassays to detect levels of total and oligomeric forms of α-syn, and phosphorylated and phosphorylated oligomeric forms of α-syn, within body fluids, in an attempt to find a biomarker that will differentiate between these disorders. Levels of these 4 different forms of α-syn were measured in post mortem samples of ventricular cerebrospinal fluid (CSF) obtained from 76 patients with PD, DLB, PSP or MSA, and in 20 healthy controls. Mean CSF levels of total and oligomeric α-syn, and phosphorylated α-syn, did not vary significantly between the diagnostic groups, whereas mean CSF levels of phosphorylated oligomeric α-syn did differ significantly (p<0.001) amongst the different diagnostic groups. Although all 4 measures of α-syn were higher in patients with MSA compared to all other diagnostic groups, these were only significantly raised (p<0.001) in MSA compared to all other diagnostic groups, for phosphorylated oligomeric forms of α-syn. This suggests that this particular assay may have utility in differentiating MSA from control subject and patients with other α-synucleinopathies. However, it does not appear to be of help in distinguishing patients with PD and DLB from those with PSP or from control subjects. Western blots show that the principal form of α-syn within CSF is phosphorylated, and the finding that the phosphorylated oligomeric α-syn immunoassay appears to be the most informative of the 4 assays would be consistent with this observation.

© 2011 Elsevier Inc. All rights reserved.

Introduction

Idiopathic Parkinson's disease (PD) is one of several neurodegenerative disorders that can present with similar clinical symptoms, particularly parkinsonism which is a combination of tremor, rigidity and bradykinesia. Progressive supranuclear palsy (PSP), corticobasal syndrome (CBS) and multiple system atrophy (MSA) are neurodegenerative conditions that are neuropathologically distinct entities, but show clinical overlap with PD. Because of the prominent clinical features they show in addition to parkinsonism, they are often described as "atypical" Parkinsonian syndromes.

In vivo diagnosis of PD and atypical Parkinsonian disorders relies on clinical criteria (Poewe and Wenning, 2002). Although none of these disorders is currently curable, it is important to make the correct diagnosis as early as possible since the symptomatic therapeutic approaches differ, and future (causative) therapies might be targeted directly against the underlying pathological process in each of these disorders. Reliable, early clinical diagnosis is also crucial for correct classification of patients within clinical trials (Schlossmacher and

* Corresponding author. Fax: +44 1524 593 192.
  E-mail address: d.allsop@lancaster.ac.uk (D. Allsop).
  Available online on ScienceDirect (www.sciencedirect.com).

Mollenhauer, 2010). Nonetheless, clinical diagnosis of PD is often imprecise, particularly during the early stages of the illness. Indeed, clinicopathological studies have shown that only 69–70% of people with autopsy-confirmed PD had, in life, at least two of the cardinal clinical signs of the disease, and 20–25% of people with two of these symptoms had a pathological diagnosis other than PD (Hughes et al., 1992, 2001). There is clearly an urgent need to develop a biomarker for PD and the related disorder of Dementia with Lewy bodies (DLB) which will not only distinguish these disorders from normal people, but also from patients with other parkinsonian and/or dementing syndromes. Considerable effort therefore currently goes into the development of biomarkers for PD and the atypical parkinsonian disorders that would reliably allow the clinician to distinguish between them at an early stage.

PD and DLB are both characterised pathologically by the deposition of aggregated forms of α-synuclein protein (α-syn) in the brain in the form of neuronal cytoplasmic inclusions (Lewy bodies, LBs) and dystrophic processes (Lewy neurites, LNs) (Spillantini et al., 1997, 1998). In PD, α-syn pathology is principally found in brain stem and mid brain structures (substantia nigra, locus caeruleus, dorsal motor vagus, and nucleus of Meynert) (Spillantini et al., 1997), whereas in DLB the similar α-syn changes are focussed on regions such as cingulate cortex, parahippocampal gyrus and amygdala (Spillantini et al., 1998). LBs and LNs contain a misfolded, fibrillar and phosphorylated form of α-syn (Anderson et al., 2006; Spillantini et al., 1997). In demented PD patients (PDD), there is a 'spread' of α-syn pathology into cortical structures, and PD, PDD and DLB may form a continuum of disease. Pathological changes also involving α-syn, but chiefly in glial cells, characterise MSA. Collectively, PD, DLB and MSA are often referred to as 'α-syncleinopathies' (Spillantini et al., 1998). PSP and CBS on the other hand are tauopathies.

We, and others, have previously reported that α-syn can be detected within cerebrospinal fluid (CSF) and plasma (El-Agnaf et al., 2003, 2006; Tokuda et al., 2006, 2010). This extracellular form of α-syn seems to be secreted from neuronal cells by exocytosis (Emmanouilidou et al., 2010; Lee et al., 2005) and could play an important role in cell-to-cell transfer of α-syn pathology in the brain (Angot and Brundin, 2009). Consequently, levels of α-syn within plasma and/or CSF might therefore serve as a biomarker for PD, and other α-synucleinopathies (i.e. DLB, MSA). Here, we have tested whether ventricular post mortem CSF measures of α-syn can predict the presence or amount of α-syn pathology within the brain in α-synucleinopathies, and can differentiate the α-synucleinopathies from each other, as well as from other parkinsonian disorders, such as progressive supranuclear palsy (PSP), which are characterised by tauopathy. Moreover, because pathological investigations have demonstrated that the aggregated α-syn within LBs and LNs is phosphorylated (at Ser 129) (Anderson et al., 2006; Fujiwara et al., 2002; Obi et al., 2008), we have argued (Foulds et al., 2010) that these modified, pathological forms of the protein ought to more accurately reflect the fundamental neuropathology of PD, and that measurements of phosphorylated α-syn within CSF might provide a more direct marker of α-syn pathology in the brain (akin to measurement of tau phosphorylated at Ser 181 (ptau-181) as an index of neurofibrillary pathology in AD (see Blennow and Hampel, 2003 for review)), than the more straightforward measures of 'total α-syn' which most previous assays (for example, El-Agnaf et al., 2003, 2006; Tokuda et al., 2006, 2010) have been limited to.

Materials and methods

All CSF samples and brain tissues had been collected with full Ethical permission, following donation by next of kin, and were kindly provided by the Parkinson's Disease UK Brain Bank (PDUKBB) and Queen Square Brain Bank (QSBB), except for one MSA case from Manchester Brain Bank (MBB). Clinical diagnoses had been made locally by the referring specialist Neurologist in care of the patient. Nonetheless, in all instances, the clinical diagnosis had been confirmed pathologically by Neuropathologists within their respective tissue banks. For PDUKBB cases, clinical information and neuropathological reports were available on PDUK web site. For QSBB and MBB cases relevant information was available locally. All clinical and pathological diagnoses were made in accordance with internationally recognised criteria.

Samples of CSF were obtained at post mortem from 96 individuals (Table 1), 85 were provided by the PDUKBB, 10 by QABB and one from MBB. CSF was drawn directly at post mortem from the subarachnoid space and/or lateral ventricles and immediately frozen and stored at −80 °C pending analysis. The post mortem delay time between death and obtaining/freezing CSF was variable, ranging from 2 to 96 h, though 62% of samples had been collected within 24 h of death and only 15% after 48 h of death.

Of the 85 samples from PDUKBB, 39 were from patients clinically diagnosed as having PD, 17 patients had DLB, 7 had PSP, 4 had MSA and 18 were controls. Of the 10 samples from QSBB, 5 had PSP, 3 had MSA and 2 were controls. The sample from MBB had MSA. Twenty six of the PD patients were anecdotally reported in their clinical histories as suffering from dementia (PD Dem) and/or cognitive impairment (PD Cog), whereas no evidence of cognitive impairment or dementia had been reported in the other 13 patients who were therefore considered to be cognitively unimpaired (PD nonD). All patients with PSP had classical Steele–Richardson syndrome. All patients with MSA had striatonigral degeneneration (SND) subtype except one with a mixed subtype. Formal neuropsychological testing had not been performed for most of the PD and DLB cases, and MMSE scores were therefore generally not available. One of the QSBB PSP cases scored 23/30 on MMSE and 3 others from PDUKBB were reported as suffering from dementia, but the remaining PSP cases, and all the MSA and control cases had been considered to display no cognitive impairment, or had normal MMSE scores (where available).

Although, overall, age at onset, age at death and duration of illness differed significantly between PD, DLB, PSP, MSA and control groups ($F_{3,72} = 2.95$, p = 0.039, $F_{4,95} = 2.48$, p = 0.05, $F_{3,72} = 4.55$, p = 0.006, respectively) (Table 1), post hoc Tukey test showed no significant differences in any of these measures between any of the diagnostic groups, probably because of the small sample sizes involving PSP and MSA groups, particularly in respect of disease duration (Table 1). There were no significant differences between PD, PDD or DLB groups ($F_{2,52} = 0.43$, p = 0.654; $F_{2,53} = 2.40$, p = 0.100; $F_{2,52} = 0.845$, p = 0.435, respectively).

Paraffin sections (6 μm) of frontal and cingulate cortex, hippocampus and temporal cortex, amygdala and parahippocampus, and substantia nigra were obtained from the PDUKBB and QSBB from the same PD, DLB, PSP and MSA patients, wherever possible. However, sections were only available from 6 of the 20 control subjects (4 from PDUKBB and 2 from QSBB (Table 1).

Table 1
Selected clinical and demographic details of cases studied.

Group	Gender	Age at onset (year)	Age at death (year)	Duration (year)
All PD (n = 39)	29M, 13F	64.2 ± 11.8	78.4 ± 6.7	14.2 ± 7.8
PD (n = 13)	10M, 3F	66.1 ± 11.7	79.0 ± 6.5	12.9 ± 6.6
PDD (n = 26)	19M, 10F	63.3 ± 12.0	78.1 ± 6.9	14.8 ± 8.4
DLB (n = 17)	14M, 3F	62.4 ± 8.2	74.0 ± 7.5	11.8 ± 6.9
PSP (n = 12)	10M, 2F	73.5 ± 6.9	80.7 ± 7.9	6.6 ± 3.8
MSA (n = 8)	4M, 4F	64.3 ± 7.6	70.9 ± 7.4	7.6 ± 2.9
Controls (n = 20)	13M, 7F	na	77.9 ± 12.1	na
[a]Controls (n = 6)	5M, 1F	na	73.3 ± 12.4	na

[a] Those 6 of the 20 control cases for which paraffin sections were available.

Biochemical methods

Preparation of recombinant α-syn

Recombinant α-syn (without any purification tag) was prepared at Lancaster University from *E. coli* using the following protocol. pJEK2 was used to transform FB850, a *rec* A⁻ derivative of BL21 (DES) pLysS. FB850 carrying this plasmid was grown in an 800 ml batch culture and protein expression was induced through the addition of isopropyl-β-D-thiogalactopyranoside (IPTG). A protein with a molecular weight of ~17 kDa started to accumulate in the cells 30 min after induction and reached maximum levels after 150 min. Immunoblot analysis identified this protein as α-syn using an anti-α-syn mouse monoclonal antibody (MAb 211, from Santa Cruz Biotechnology, Santa Cruz, CA, USA). After a 3 h induction, the suspension was centrifuged, and the cells resuspended in buffer. The cells were lysed by sonication, and then cell debris and insoluble material was removed by centrifugation at 4 °C for 1 h at 30,000 rpm. α-Syn was extracted from the supernatant by ammonium sulphate precipitation, then purified using two chromatography columns; mono Q and Superose 6. After purification, 5 µg of protein ran as a single band when observed on a Coomassie blue-stained SDS gel, corresponding to monomeric α-syn.

Preparation of phosphorylated α-syn

Phosphorylated α-syn was prepared from recombinant α-syn as described previously (Sasakawa et al., 2007).

Preparation of oligomeric forms of α-syn

To prepare a standard for the oligomeric α-syn immunoassay, the recombinant protein was oligomerised by incubation at 45 µM in phosphate-buffered saline (PBS) in an orbital shaker at 37 °C for 5 days, and the monomer and oligomer were separated by size exclusion chromatography. A sample (0.5 ml) of pre-aggregated α-syn was loaded onto a Superose 6 column (44×1 cm) connected to a fast protein liquid chromatography (FPLC) system (Atka Purifier, GE Healthcare) and eluted with running buffer (PBS) at a flow rate of 0.5 ml/min. Absorbance of the eluate was monitored at 280 nm and fractions of 1 ml were collected and protein concentration determined.

To prepare a standard for the phosphorylated oligomeric α-syn immunoassay, the phosphorylated protein was allowed to aggregate by incubation at 50 µM in PBS in an orbital shaker at 37 °C for 5 days. Aggregation of the protein was confirmed by thioflavin T assay (see Supplementary data). In this case, the amount of sample available was too small to fractionate by size-exclusion chromatography.

Immunoassays

We have already established immunoassays for the measurement of 'total' and 'soluble oligomeric' forms of α-syn in human biological fluids, including blood plasma and CSF (El-Agnaf et al., 2003, 2006; Tokuda et al., 2006), but these methods have been further optimized here.

Total α-syn

An ELISA plate (Iwaki) was coated with 100 µl/well of anti-α-syn monoclonal antibody 211 diluted 1:1000 (Santa Cruz Biotechnology, Inc., Santa Cruz, CA) (0.2 µg/ml) in 50 mM NaHCO₃, pH 9.6, and incubated at 4 °C overnight. The wells were then washed 4 times with PBS containing 0.05% Tween-20 (PBS-T), and incubated for 2 h at 37 °C with 200 µl/well of freshly prepared blocking buffer (2.5% gelatin in PBS-T). The plate was washed again 4 times with PBS-T and 100 µl of the assay standard or CSF samples were added to each well, (each CSF sample was diluted 1:40 with PBS), and the assays were performed in triplicate. Following this, the plate was incubated at 37 °C for 2 h. After a repeat washing with PBS-T, 100 µl/well of the detection antibody, anti-α/β/γ-synuclein FL-140 (Santa Cruz Biotechnology, Inc., Santa Cruz, CA), dilution 1:750 (0.27 µg/ml) in blocking buffer was added, and the plate was incubated at 37 °C for 2 h. After another wash with PBS-T, the plate was incubated with 100 µl/well of secondary antibody (goat anti-rabbit HRP (Sigma), dilution 1:10,000 in blocking buffer at 37 °C for 2 h. The plate was then washed again with PBS-T before adding 100 µl/well of Sure Blue TMB Microwell Peroxidase Substrate (KPL, USA) and leaving the colour to develop for 30 min at room temperature. Finally 100 µl/well of stop solution (0.3 M H₂SO₄) was added and absorbance at 450 nm was determined. Recombinant monomeric α-syn was used to create a standard curve (Fig. 1a).

Oligomeric α-syn

The microtitre plate was coated and blocked using the same method as the assay for 'total α-syn'. The wells were then washed 4 times with PBS-T and 100 µl of the CSF samples (diluted 1:25 with PBS) or assay standard (oligomeric α-syn) was added to each well, in triplicate. Following this, the plate was incubated at 37 °C for 2 h. After a repeat wash with PBS-T, 100 µl/well of the detection antibody, biotinylated anti-α-synuclein 211 (diluted 1:1000 in blocking buffer) was added, and the plate was incubated at 37 °C for 2 h. After another wash with PBS-T, the plate was incubated with 100 µl/well of streptavidin-europium, diluted 1:500 in streptavidin-europium buffer (Perkin Elmer) and shaken for 10 min. After a further 50 min agitation on a rotating platform, the plate was washed again with PBS-T, before adding 100 µl/well enhancer solution (Perkin Elmer). Finally, the plates were read on a Wallac Victor² 1420 multi-label plate reader, using the time-resolved fluorescence setting for europium.

Oligomeric α-syn was used to create a standard curve (Fig. 1b). The specificity of this assay towards aggregated forms of α-syn was confirmed (the α-syn monomer gave no significant signal).

Phosphorylated α-syn

The antibody-sandwich immunoassay for 'total' α-syn was modified to detect only phosphorylated forms of the protein by replacing the 211 phospho-independent capture antibody with polyclonal anti-α-synuclein N-19 (Santa Cruz Biotechnology, Inc., Santa Cruz, CA, USA), diluted 1:3000 (0.07 µg/ml). The phospho-dependent rabbit monoclonal antibody, Phospho (pS129) Antibody (Epitomics Inc., CA, USA), used at a dilution of 1:3000, was the chosen detection antibody. This antibody only detects α-syn phosphorylated at Ser129. The preferred secondary antibody was human serum absorbed goat anti-rabbit HRP, 1:3000 (KPL, USA, rehydrated in 1 ml H₂O). This assay did not detect non-phosphorylated recombinant α-syn.

Oligomeric, phosphorylated α-syn

The antibody-sandwich ELISA for 'oligomeric' α-syn was modified to detect only phosphorylated, oligomeric forms of the protein, by replacing the 211 phospho-independent capture antibody with the phospho-dependent rabbit monoclonal antibody, Phospho (pS129) (Epitomics, Inc., CA, USA), used at a dilution of 1:3000. The detection antibody was biotinylated Phospho (pS129) at a dilution of 1:400. Recombinant, oligomerised, phosphorylated α-syn (oligo-pS-α-syn) was used to generate a standard curve (Fig. 1d). This assay did not detect the monomeric form of pS-α-syn.

Immunoblotting

According to the measures of total and oligomeric α-syn within CSF, cases with relatively high and low concentrations of α-syn were